JSEE Vol. 26, No. 4, 2024 DOI: 10.48303/jsee.2024.2015698.1082

Research Paper

Effect of Non-Linearity of Stiffness during the Nucleation Phase of an Earthquake

Francis Olivier Djiogang[1*], Fidele Koumetio[2] and David Yemele[2]

1. Ph.D., Research Unit for Mechanics and Modeling of Physical Systems (UR-2MSP), University of Dschang Cameroon, Faculty of Sciences, Cameroon, *Corresponding Author; email: fdjiogang@gmail.com
2. Prof., Research Unit for Mechanics and Modeling of Physical Systems (UR-2MSP), University of Dschang Cameroon, Faculty of Sciences, Cameroon

Received: 14/11/2023
Revised: 09/06/2024
Accepted: 14/07/2024

Keywords:
Nucleation phase; Non-linearity; Anisotropy; Elasticity coefficient; Dimensional Velocity

ABSTRACT

Stiffness plays an important role during earthquake rupture dynamics. At the main slip zone, the response of the system following a solicitation is both a function of stiffness and the heterogeneity of the surroundings. This work studies the effect of heterogeneity of Earth crust, particularly the effect of spatial dependence of stiffness during the nucleation phase of an earthquake. Based on Burridge Knopoff's 1D model, we have redesigned the dynamics of an earthquake, taking into account the spatial variation of stiffness. The obtained differential system being complexity, a numerical approach was used to draw solutions to the problem. We represented the variation curves of temperature, energy and displacement as well as the speed obtained when the rigidity is constant (CS) and when the stiffness is nonlinear (NLS). Then a comparative study was conducted between the two cases. We show that, by considering the space-dependent of stiffness, the stick-slip movements occurred and a succession of oscillations with decreasing amplitude in time, separate to the case where it was considering to be constant. The non-linearity of the stiffness reveals that each oscillation is separated from the next by a coseismic phase. For non-linearities of order one and in the presence or absence of a fluid, the spatial dependence of stiffness suggests the existence of a seismic motion with decreasing amplitude, which always precedes by a steady state when the stiffness is nonlinear, which is not the case when the stiffness is constant; moreover, the amplitude of the movement decreases.

How to cite the article:
DJIOGANG, F. O., Fidèle, K. and YEMELE, D. (2024). Effect of non-linearity of stiffness during the nucleation phase of an earthquake. *Journal of Seismology and Earthquake Engineering*, *26*(4), 1-24. doi: 10.48303/jsee.2024.2015698.1082

1. Introduction

Earthquakes are the consequences of internal activity of earth. They are for the most part characterized by three phases: nucleation, proper manifestation and return to calm. Given the complexity of its dynamics and numerous hypotheses that are involved in its solution (Florido et al., 2015), the prediction and understanding of its phenomena remains a challenge for scientists. One of the reasons why the prediction and understanding of earthquakes remains problematic is the fact that, during numerical simulations in the laboratory, these rupture dynamics requires several assumptions ranging from the geometry of the faults, to the initial conditions on the initial stress in rocks before an earthquake to rock properties, including shear and compression wave velocities and densities (Harris et al., 2018). Another reason why the prediction of earthquakes is so complex is that during the nucleation phase of an earthquakes and seismic events, several changes in the structure of the earth are observed, such as variation in the electrical conductivity of the medium as well as the stress; modification of shape of the seismic wave during its propagation, variation of random concentration in groundwater, earth and air, fluctuation of ground water level's, thermal anomalies, electromagnetic variation near and above Earth's (Konga et al. 2017, 2020; Florido et al., 2015; Jordan et al., 2011). All these theories issued to better understand earthquakes, the theories conducted during the pre-seismic phase remain the most important for the understanding of earthquakes. Many of the theories put forward by the pioneers in seismic fields only took into account the fact that seismic waves propagate in isotropic media with fixed characteristic parameters. The introduction of non-homogeneity of the surroundings and anisotropy has in recent years opened many new issues in understanding the propagation of seismic waves. Olami et al. (1992) were the first to introduce the concept of anisotropy hypothesis in their work. Kostic et al. (2014) worked on the 1D dynamics of the Burridge-Knopoff model (Burridge & Knopoff, 1967) normal static pressure with single-block model using Dieterich-Ruina's rate- and state-dependent friction law by taking into account perturbation of velocity relaxation coefficient and elastic constants. Their work allowed highlighting a chaotic and deterministic behavior of the system due to the fact that we considered small variations of oscillations around the equilibrium position. Moreover, they showed the existence of one or two periodic variables and two different possible scenarios of chaos (one for the limit perturbations of the amplitudes and the other when the angular frequency was considered constant). By varying the physical properties of water, Urata et al. (2015) studied the effect of transitional phase of water on the dynamics rupture of fault with thermal pressurization. They were able to highlight that by changing the physical properties of water, the total slip of the system was greater compared to the case where the physical properties were constant. In addition, they showed that varying the water properties resulted to a decrease in total slip for large values of stress at depth and as well as for small slip zones. Wang (2017) evaluated the effect of friction and viscosity during the nucleation phase of an earthquake. His work showed that both friction and viscosity cause an increase in natural period of the system; and viscosity increases the time duration of slip motion. Konga et al. (2017) modeled the thermal energy produced by friction at the fault lip in the 1D domain. Their work proved that both thermal energy and temperature grew rapidly with time and that for aperiodic motions, the temperature profile was constant over time. Based on the one-dimensional Burridge-Knopoff model, Konga et al. (2020) found the effect of the variation of the viscosity coefficient on the frictional thermal energy at the fault lip, highlighting that thermal energy was maximum when the seismic wave value was maximum. Motchongom et al. (2022), on the basis of Burridge-Knopoff model develop the dynamics of two blocks by taking into account the periodic perturbation of the stress and the friction parameter. In this work, they showed that a periodic distur bance has the effect of increasing the duration of the inter-seismic phase. Furthermore, they demonstrated that stick-slip motion with a multitude of periods was emphasized, as well as chaotic irregular motion when changing the frequencies. The works of Gomberg and Davis (1996), Brodsky et al. (2000), Gomberg and Reasenberg (2001)

suggested the existence of a small event preceding the passage of the seismic wave. Perfettini et al. (2003a, 2003b) studied the influence of normal and tangential stress on the one-dimensional and two-dimensional dynamics of the seismic fault and obtained that the Coulomb failure model predictions were reasonably close to those deduced using a more realistic failure model.

According to Ray and Viesca (2019), the properties of friction are likely varying in space for large faults. This variation in space of the physico-chemical properties of the quantities characterizing the fault is called heterogeneity. A large number of works in the literature have introduced the concept of heterogeneity in the dynamics of an earthquake. Thus, Perfettini et al. (2003a, 2003b) introduced heterogeneity to describe the scaling law of the slip weakening rate at the onset of instability using a two-dimensional fault model. In addition, the authors showed that large faults are always more unstable than small faults. Ampuero et al. (2006) investigated the effect of fault structure and heterogeneity on basic seismicity properties. They highlight the relationship that exists between the statistical properties of the stress and the properties of the macroscopic source, such as the size of the rupture, the seismic moment, the drop in apparent stress and the radiated energy of an earthquake. They also showed that stress correlation length plays an important role, appearing as a characteristic short length in the scaling behavior of macroscopic source properties and may mask or may be confused with the signature of the nucleation process. Considering that slip and system state are functions of friction as well as normal stress, Ray and Viesca (2017) investigated on the slip instability on fault dynamics. From their works, during instability development, slip rate and state evolution can be attracted to develop in the manner of the self-similar solution, which is also confirmed by solutions to initial value problems for slip rate and state. A few months later, Ray and Viesca (2019) consider a rate-and -state dependent fault friction in which the characteristic wavelength for the property variations is a problem parameter for homogenization of fault frictional properties to show that the dynamics of earthquake-nucleating facilities is controlled by the properties' spatial distribution. Lebihain et al. (2021) studied in 2D the effect of heterogeneous weakening rates along the faults during earthquake nucleation. We find that the interplay between frictional properties and the asperity size gives birth to three instability regimes (local, extremal and homogenized), each related to different nucleation scenarios, and that the influence of heterogeneities at a scale far lower than the nucleation length can be averaged. By introducing the coalescence of microslip during the nucleation phase, Schar et al. (2021) showed that when the correlation length is large, the growth of the slip patch is continuous. They also established that nucleation by coalescence is also observed on stochastic interfaces with small correlation length. In accordance with this last one, we show that its expectation follows a logistical function, which allows us to predict the strength of the interface well before failure occurs. All these works were done under the assumption that the surroundings were homogeneous. However, anisotropy and heterogeneity are important factors in the fault rupture process. According to Lebihain et al. (2021), the knowledge of the nucleation process along a heterogeneous interface remains incomplete. Thus, in order to explain the high frequency of seismic radiation and the high mobility of faults observed during large earthquakes, Mase and Smith (1987) showed that a heterogeneous stress drop and an irregular slip rate were necessary. In a similar way, Harris et al. (2021) modeled earthquake dynamics rupture in 3D based on geological and geodesic models, and showed that rock properties affect the locations and amount of slip produced in our large earthquake simulations. The crucial factors that control the rupture behavior in our modeling are earthquake nucleation locations, fault geometry, and data that reveal where the fault system is moving. All these works rightly demonstrate the importance of anisotropy and heterogeneity of surroundings in the rupture dynamics of a fault. Bearing in mind all the foregoing that, in this article, we will study the effect of non-linearity of rigidity on the nucleation phase of an earthquake. For this, we will proceed through a comparative study of the cases where the stiffness is constant (CS) and the cases when the stiffness is nonlinear (NLS) for different friction function. Considering where the stiffness is

constant (CS) and the case where it depends on space (NLS), we will extend our comparative study to the different cases of friction functions namely the TP law, the SW law and the VW law, in order to present the most stable for our model. We will try to highlight the existence of a cosmic phase characteristic of seismic manifestations.

2. Description and Mathematical Modeling

The system under study consists of a block of mass M placed on a fixed support. The mass M is connected to a tectonic plate by a spring of stiffness k. The tectonic plate is in translational motion with velocity as shown in Figure (1). The block is tracked by the driving force $k\nu_p t$. The whole is subjected to a frictional force opposite to the movements of block $F(u,\nu)$, which is proportional to the relative displacements of block u and the relative velocity $\nu = du/dt$ of the block mass M. Taking into account the geometry of the fault as well as the presence of a fluid, the mass M will also be subjected to a viscosity force proportional to the velocity and defined by $\Phi(\nu) = \eta\nu$, where η is the viscosity coefficient (Figure 1). Considering all the forces involved, and using the center of inertia theorem on the mass M, the differential equation that governs the dynamics of motion is written:

$$M\frac{d^2u}{dt^2} = -ku - \Phi(\nu) - F(u,\nu) + k\nu_p t \qquad (1)$$

In the software literature, there are several models of the frictional forces including a slip weakening friction law (denoted by TP), the displacement softening-hardening friction law (denoted by SH), slip-weakening friction law (denoted by SW) and velocity-weakening friction law (denoted by VW).

The SH law defined by: $F(u) = F_0 \exp \times (-(u^2 - u_c^2)/c)$, with and are constants used by Cao and Aki (1984, 1986), and defining respectively a characteristic displacement and a constant that has dimension of length. The VW (Wang, 2017) law defined by: $F(v) = F_0/(1+v/v_c)$, where v_c is the characteristic velocity, when SW (Konga, 2020) law is: $F(u) = F_0/(1+u/u_c)$, with u_c a constant. TP law is given by: $F(u) = F_0\exp(-u/u_c)$, with a constant. In all these relations, F_0 is a constant having the dimension of a static force.

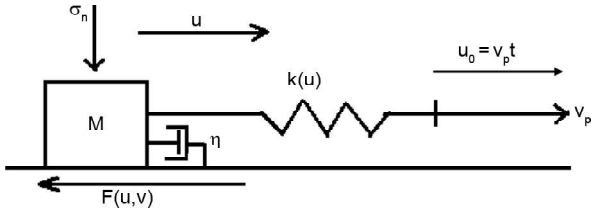

Figure 1. 1D model of earthquake nucleation with nonlinear stiffness.

Several works (Wang, 2017, Konga et al., 2020 and many others) have conducted comparative studies (quantitative and qualitative) across the different laws in order to derive the most stable one. Additional experimental and theoretical work has shown the effect of the u_c factor during the nucleation phase of an earthquake. Accordingly, Wang (2017) established that for the TP law, the frictional force decreases more swiftly for small values of u_c. However, for large values of u_c, the frictional force grows fastest and then decays for larger and larger values of u_c. Many other studies such as Marone and Saffer (2015), Wang (2016a, 2016b) and Konga et al. (2020) have been conducted by changing friction laws and considering the variation of u_c. Their studies revealed that for small values of u_c, there exists a reduced form (limited expansion) of the friction coefficient. Taking into account the different expressions formulated above, the differential equation that governs the dynamics system for the TP law is written as:

$$M\frac{d^2u}{dt^2} = -k\left(u - \nu_p t\right) - \eta\nu - F_0\exp(-u/u_c) \qquad (2)$$

Equation (2) has been studied by several authors (Wang, 2017; Wang, 2016 (a, b); Konga, 2020; Carlson & Langer, 1989, etc.). Considering the internal structure of the earth crust's which is non-homogeneous and anisotropic (Sato & Fehler, 2009; Olami et al., 1992), several hypotheses have been made about the dynamics of the system when the stiffness varies in time and space (Olami et al., 1992). Thus, Tanekou et al. (2020) modeled the dynamics of an earthquake at fractional order by assuming the nonlinear stiffness.

Considering the anisotropy in the middle and the earth's crust, the density varies from one point to another (which is justified by the existence of the

various zones of discontinuity), we will admit and consider that the stiffness is non-linear (NLS) and dependent on the position u such as $k = k(u)$ and defined by the Equation (3).

$$k(u) = k_0 + k_1 u + k_2 u^2 + k_3 u^4 + ... \quad (3)$$

In this relation, k_0 is the uniform stiffness contribution, and the term $k_1 u + k_2 u^2 + k_3 u^4 + ...$ is a function with the same dimension as $k(u)$. Taking into account a non-linearity of one order, Equation (2) becomes:

$$M \frac{d^2 u}{dt^2} = -(k_0 + k_1 u)(u - \nu_p t) - \eta\nu - F_0 \exp(-u / u_c) \quad (4)$$

Equation (4) can be developed as:

$$M \frac{d^2 u}{dt^2} = -k_0 u + k_0 \nu_p t - k_1 u^2 + k_1 u \nu_p t - \eta\nu - F_0 \exp(-u / u_c) \quad (5)$$

In view of modeling and observing the behavior of a system during nucleation phase, real values of system are needed (Wang, 2017). For this purpose, Equation (5) is dimension to approximate a system whose quantities are easily measured during seismic events. Hence, a change of variable and the following quantities are the new normative values: $D_0 = F_0 / k_0$, $\omega_0 = \sqrt{k_0 / M}$, $U = u / D_0$, $U_c = u_c / D_0$, $V_p = \nu_p / \omega_0 D_0$ and $\tau = \omega_0 t$.

Thus, we obtain $du / dt = (F_0 / \sqrt{M k_0})\, dU / d\tau$, $d^2u / dt^2 = (F_0 / M)\, d^2U / d\tau^2$ and $V = dU / d\tau$. where k_0 is the constant or reference value of stiffness (CS) when the spring is not subjected to any action of deformation. Given the change of variable, the differential Equation (5) can be written in form of Equation (6):

$$\frac{d^2U}{d\tau^2} = -U - \eta \frac{dU}{d\tau} - \exp\left(-\frac{U}{U_c}\right) + V_p \tau - \left(\frac{\omega_1}{\omega_0}\right)^2 D_0 U^2 + \left(\frac{\omega_1}{\omega_0}\right)^2 D_0 U V_p \tau \quad (6)$$

where $\omega_0 = \sqrt{k_0 / M}$ and $\omega_1 = \sqrt{k_1 / M}$ are the constants and represent respectively the natural pulsation of the system (exciter frequency), the secondary and superior pulsations due to non-linearity of elasticity coefficient. U, V and τ represent respectively dimensionless slip, dimensionless velocity, and dimensionless time. Moreover, after the change of variable, we admit that the ratio $\eta / M\omega_0$ is equivalent to a constant η and has the dimension of the viscosity coefficient of the fluid. D_0 represents a characteristic distance, which is a function of the properties of the fault zone.

For convenience, Equation (6) becomes:

$$\frac{d^2U}{d\tau^2} = -\left[1 - \varepsilon_1^2 D_0 V_p \tau\right] U - \eta \frac{dU}{d\tau} - \exp\left(-\frac{U}{U_c}\right) + V_p \tau - \varepsilon_1^2 D_0 U^2 \quad (7)$$

With $\varepsilon_1 = \omega_1 / \omega_0$

3. Numerical Solution

Equation (7) is a differential equation that translates the dynamics of a block of mass M in a medium with a nonlinear stiffness. Equation (7) is a second-order differential equation with non-constant coefficient. The analytical solution of this equation is not easy to be solved with conventional methods, so we propose the numerical solution by four order Runge-Kutta method. Therefore, let introduce the new values $X = U$ and $dU / d\tau$, Equation (7) becomes:

$$\begin{cases} \dfrac{dX}{d\tau} = Y \\ \dfrac{dY}{d\tau} = -\left[1 - \varepsilon_1^2 D_0 V_p \tau\right] X - \eta Y - \exp\left(-\dfrac{X}{U_c}\right) + V_p \tau - \varepsilon_1^2 D_0 X^2 \end{cases} \quad (8)$$

For the case of SH law, the system of Equations (8) takes the following form:

$$\begin{cases} \dfrac{dX}{d\tau} = Y \\ \dfrac{dY}{d\tau} = -\left[1 - \varepsilon_1^2 D_0 V_p \tau\right] X - \eta Y - \exp\left(-\dfrac{X^2 - U_c^2}{C^2}\right) + V_p \tau - \varepsilon_1^2 D_0 X^2 \end{cases} \quad (9)$$

where $C^2 = c^2 / D_0^2$ characterizes a dimensionless constant.

For the case of the VW law, the system of equation that governs the dynamics of a system is written:

$$\begin{cases} \dfrac{dX}{d\tau} = Y \\ \dfrac{dY}{d\tau} = -\left[1-\varepsilon_1^2 D_0 V_p \tau\right] X - \eta Y - \left(-\dfrac{V_c}{V_c + V}\right) + V_p \tau - \varepsilon_1^2 D_0 X^2 \end{cases} \tag{10}$$

For very small displacements, the SW law is the reduced form of the limited second-order development of the TP law. Indeed, during the nucleation phase of earthquakes and for very small displacements, $F(u) = F_0 \exp(-u/u_c) \approx 1 - u/u_c + u^2/2u_c^2 + \ldots$ and $F(u) = F_0/(1+u/u_c) \approx F_0(1+u/u_c)^{-1} \approx F_0(1-u/u_c)$. This analysis justifies the fact that we only represented the TP, SW, and VW laws in our study.

Elastic and plastic deformations observed in the rock in general and at fault zone in particular are consequences of an internal energetic activity of the earth crusts. During nucleation and seismic events, several sources of energy are produced and released, the most dominant being the energy produced by friction at the fault zone (Di Toro et al., 2005; Konga et al., 2020; Djiogang et al., 2022). This energy is proportional to relative velocity v of mobility of the block of mass M and the frictional force $F(u, v)$ to which the mass M is subjected. When the ratio $\varepsilon_1 \prec\prec\prec 1$ and when $\varepsilon_1^2 = 0$, Equations (8) to (10) are reduced to the equations studied by Wang (2017) and Konga et al. (2020). Indeed, when $\varepsilon_1 = \omega_1/\omega_0 = 0$, we have two scenarios. Either $\omega_1 = 0$, and the Equation (7) becomes $d^2U/d\tau^2 = -U - \eta dU/d\tau - \exp(-U/U_c) + V_p\tau$ which is the one proposed by Wang (2017). Note that in the context of this study, this case corresponds to that where the stiffness is constant (CS, blue curve in Figures 2 to 12). Let then be $\omega_0 \succ\succ \omega_1$, and we are in the same case as in the previous case.

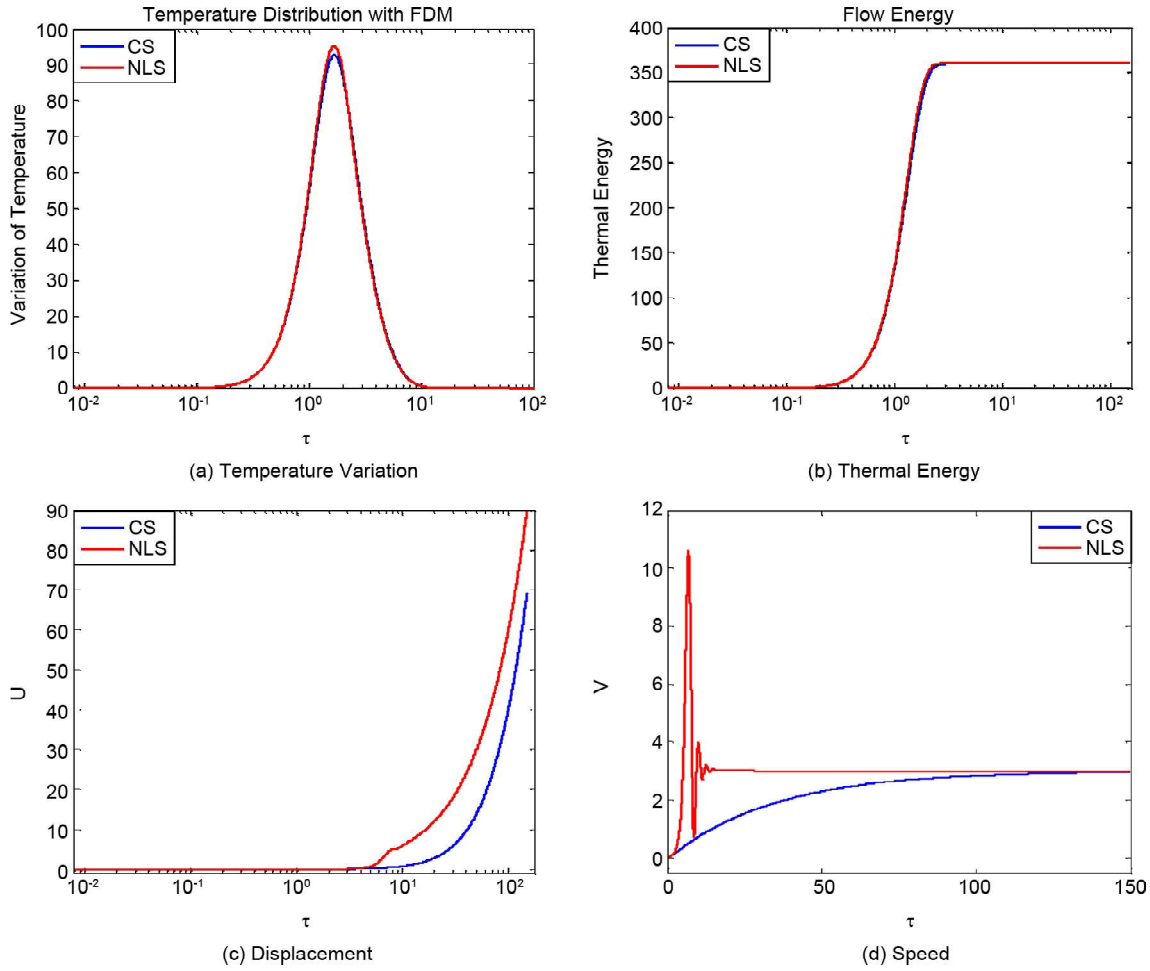

Figure 2. (a) Temperature variation, (b) thermal energy, (c) displacement, and (d) speed, for TP law for value η = 7, U_c = 0.6, D_0 = 0.5, γ = 0, v = 10^{-9}, V_p = 0.3, ε_1 = 0.7.

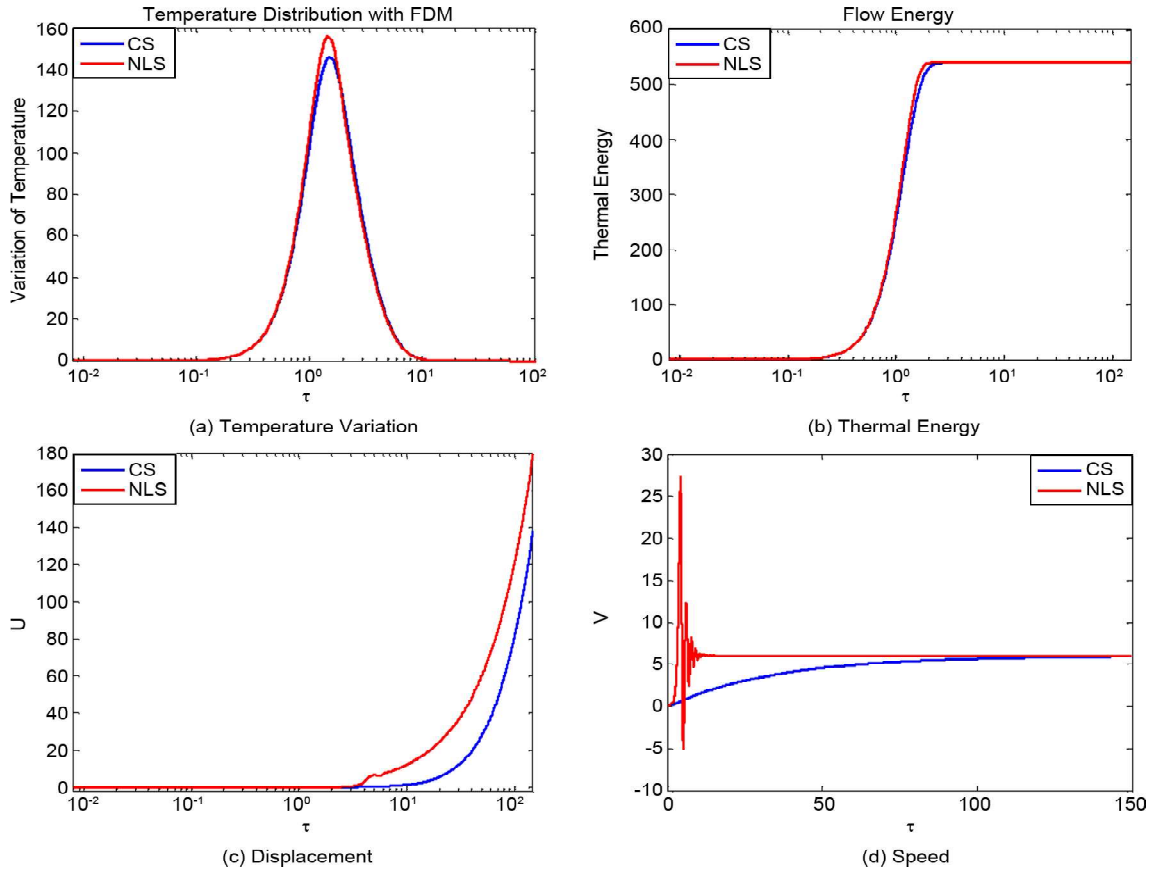

Figure 3. (a) Temperature variation, (b) thermal energy, (c) displacement, and (d) speed, for TP law for value $\eta = 7$, $U_c = 0.9$, $D_0 = 1$, $\gamma = 0$, $\nu = 10^{-9}$, $V_p = 0.6$, $\varepsilon_1 = 0.7$.

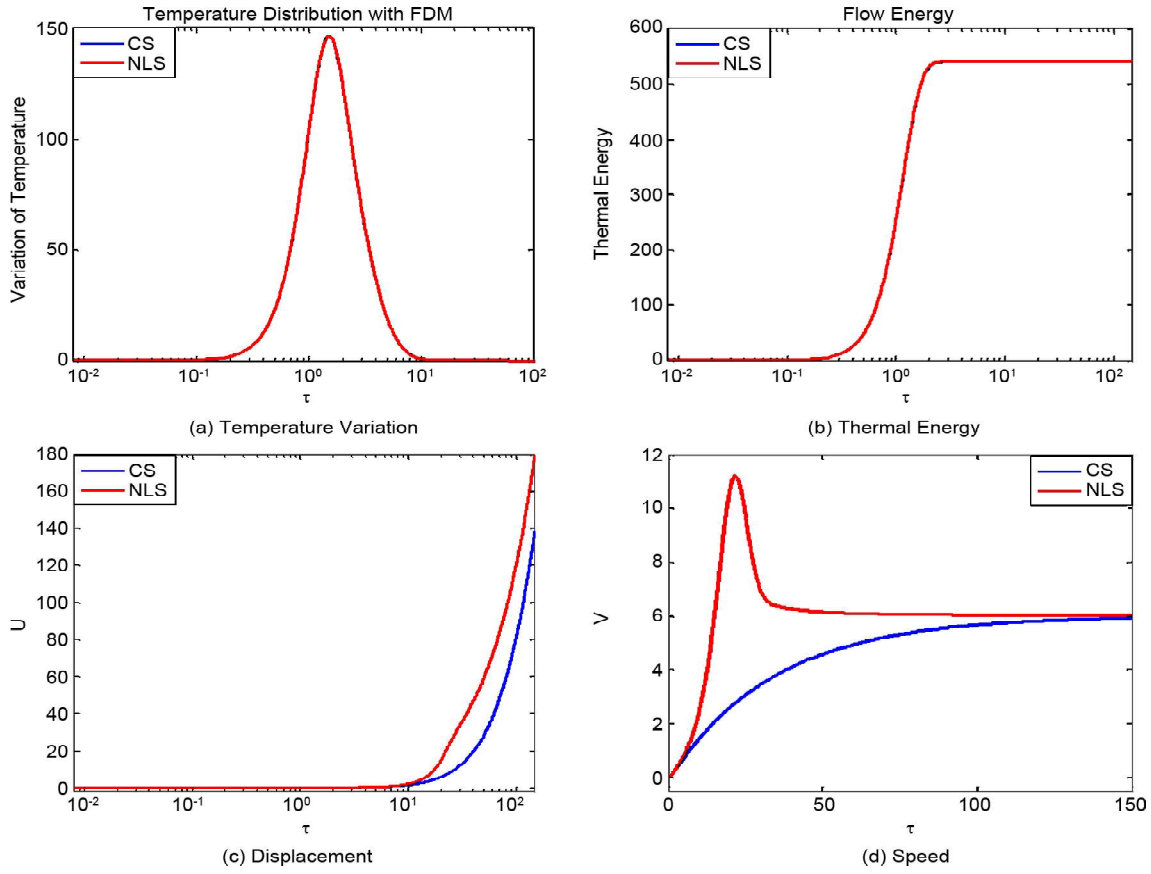

Figure 4. (a) Temperature variation, (b) thermal energy, (c) displacement, and (d) speed, for TP law for value $\eta = 7$, $U_c = 0.9$, $D_0 = 1$, $\gamma = 0$, $\nu = 10^{-9}$, $V_p = 0.6$, $\varepsilon_1 = 0.07$.

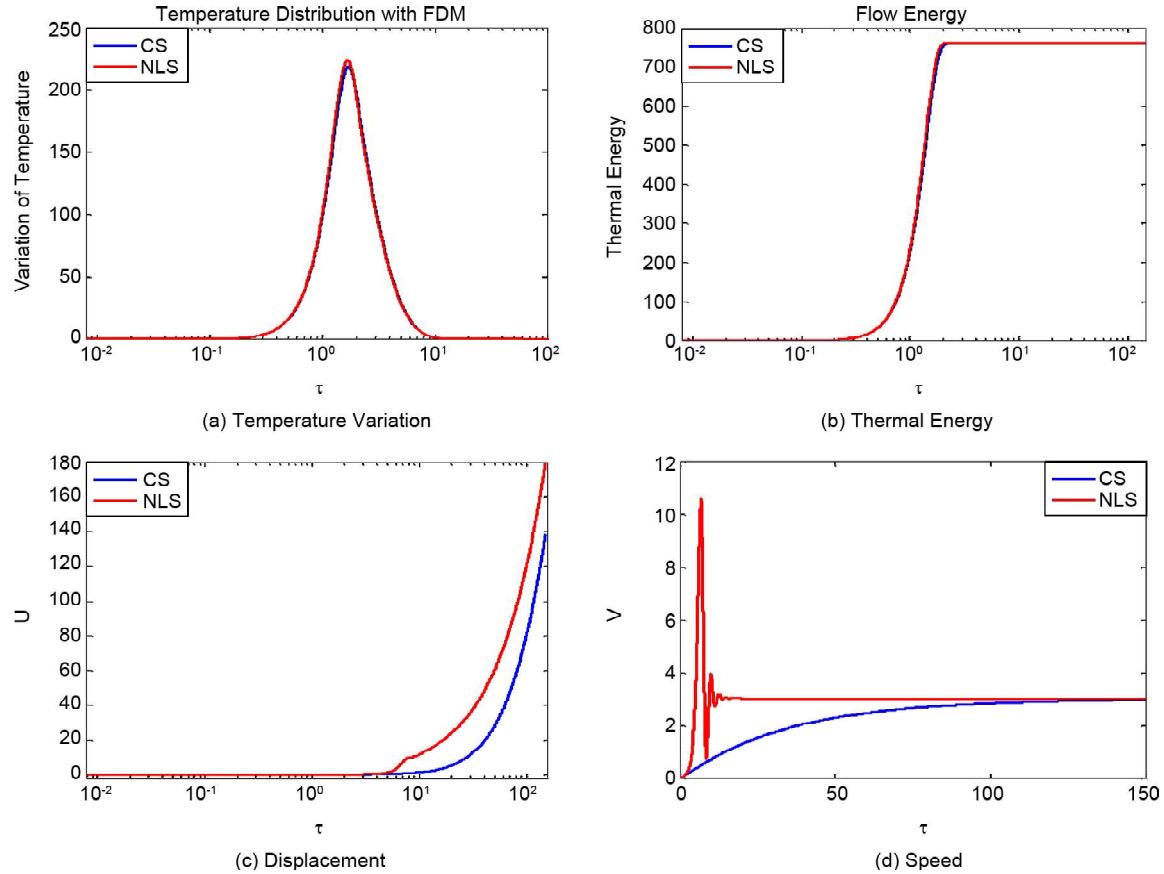

Figure 5. (a) Temperature variation, (b) thermal energy, (c) displacement, and (d) speed, for TP law for value $\eta = 7$, $U_c = 0.6$, $D_0 = 0.5$, $\gamma = 0$, $v = 10^{-9}$, $V_p = 0.3$, $\varepsilon_1 = 0.7$ and $C = 0.3$.

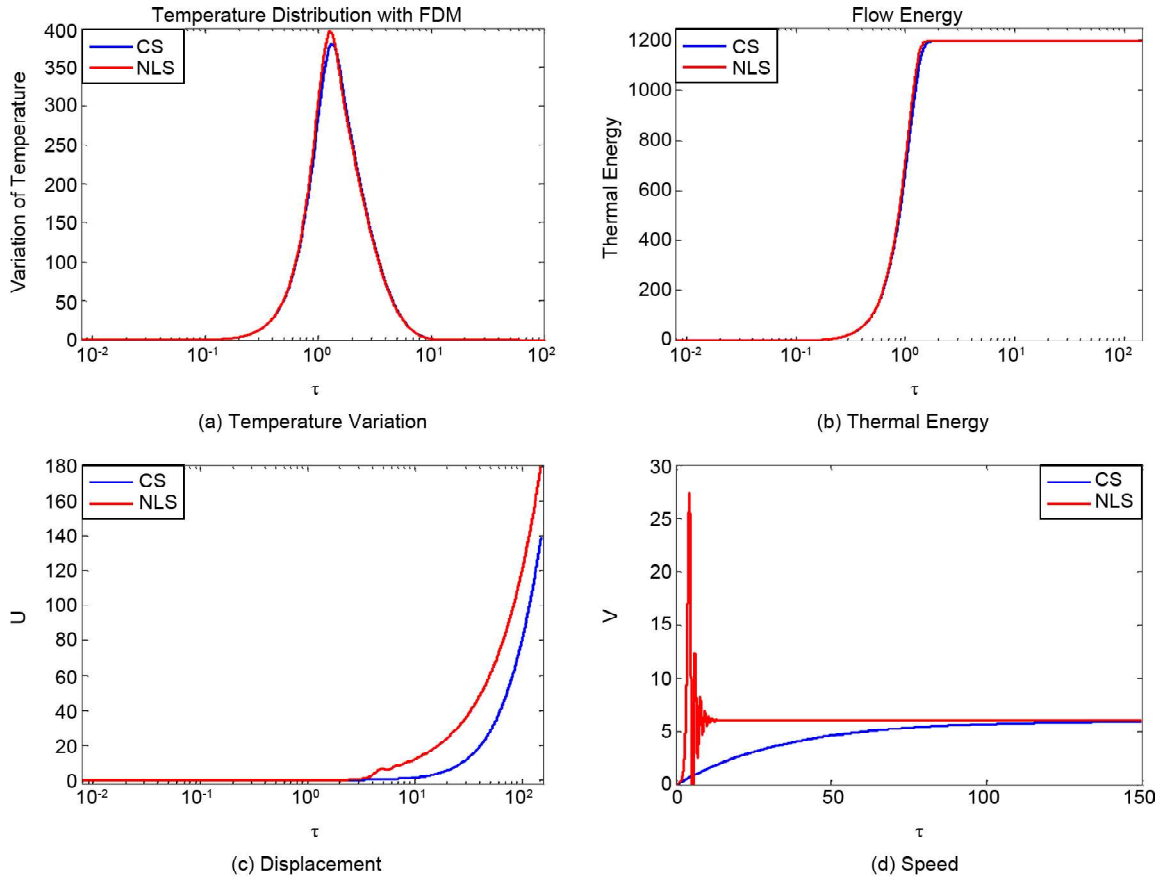

Figure 6. (a) Temperature variation, (b) thermal energy, (c) displacement, and (d) speed, for TP law for value $\eta = 7$, $U_c = 0.9$, $D_0 = 1$, $\gamma = 0$, $v = 10^{-9}$, $V_p = 0.6$, $\varepsilon_1 = 0.7$ and $C = 0.3$.

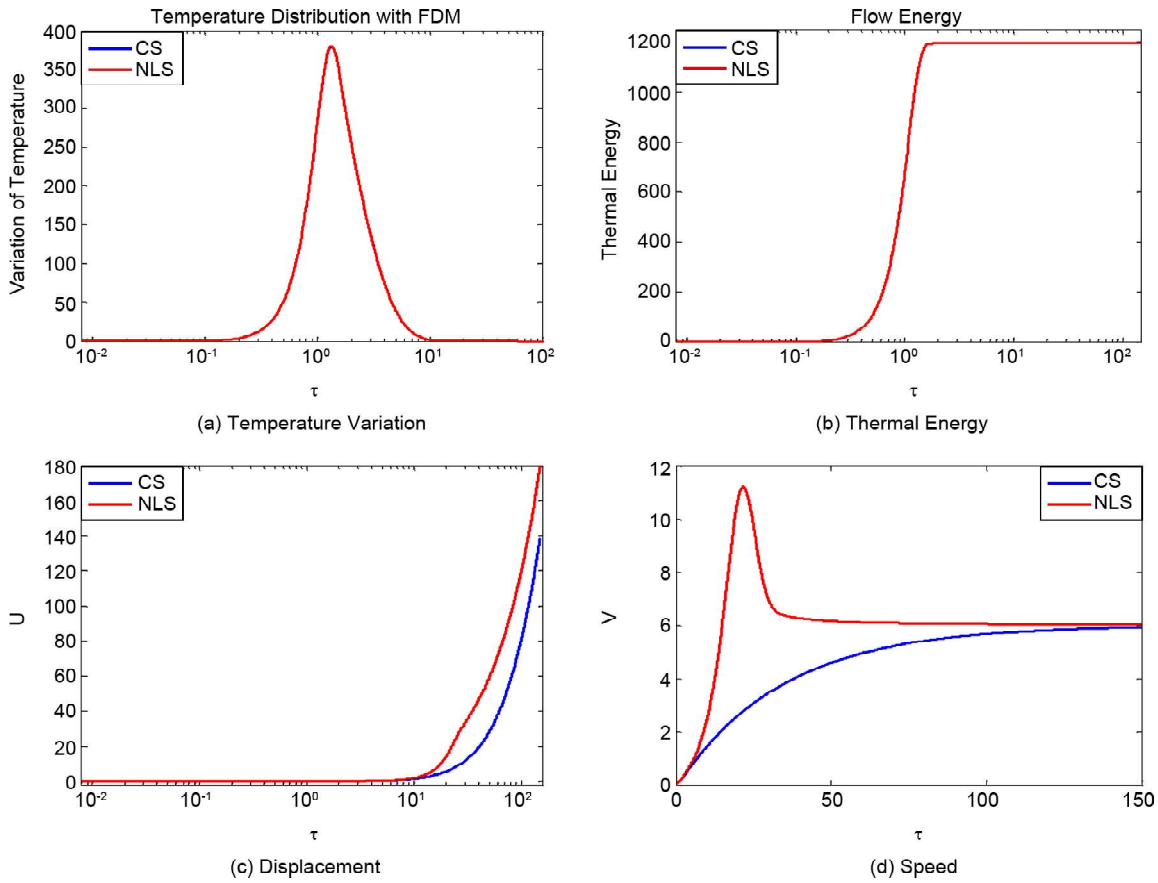

Figure 7. (a) Temperature variation, (b) thermal energy, (c) displacement, and (d) speed, for TP law for value $\eta = 7$, $U_c = 0.9$, $D_0 = 1$, $\gamma = 0$, $v = 10^{-9}$, $V_p = 0.6$, $\varepsilon_1 = 0.07$ and $C = 0.3$.

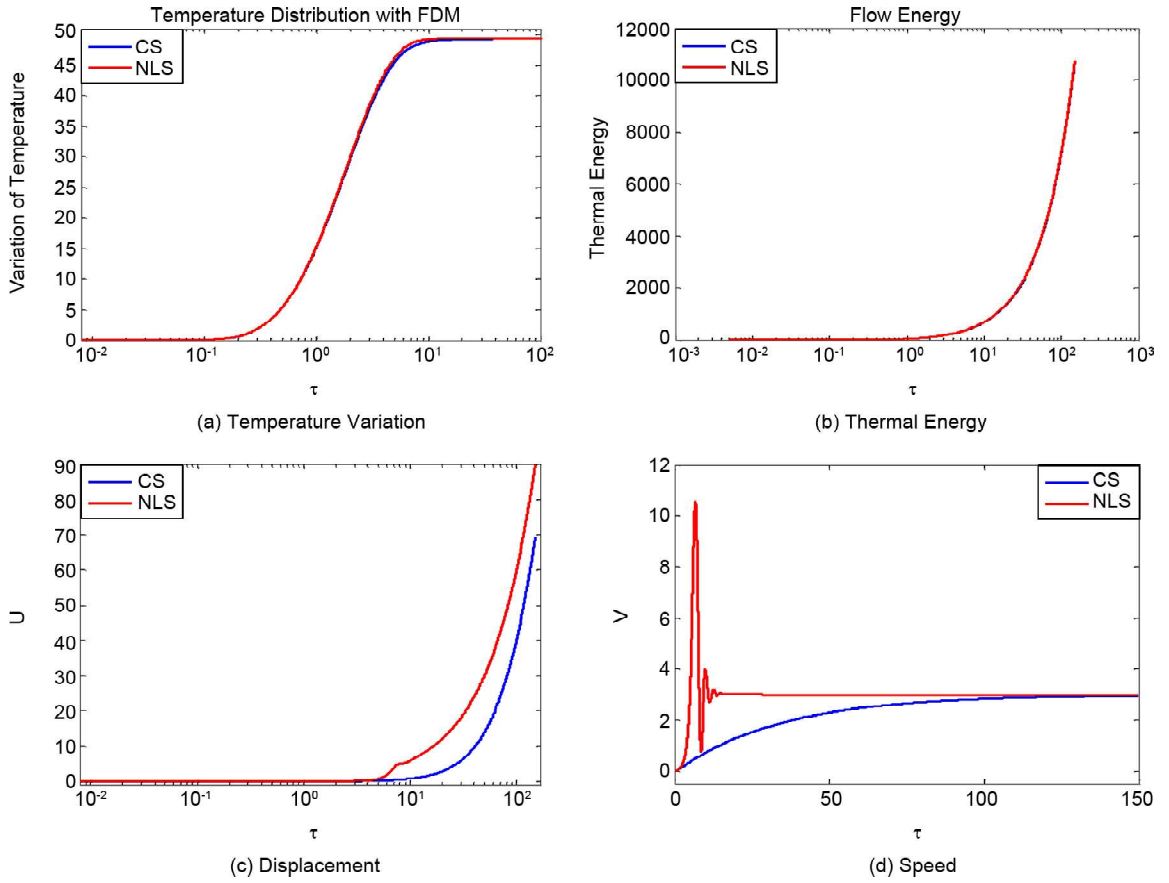

Figure 8. (a) Temperature variation, (b) thermal energy, (c) displacement, and (d) speed, for TP law for value $\eta = 7$, $U_c = 0.6$, $D_0 = 0.5$, $\gamma = 0$, $v = 10^{-9}$, $V_p = 0.3$, $\varepsilon_1 = 0.7$.

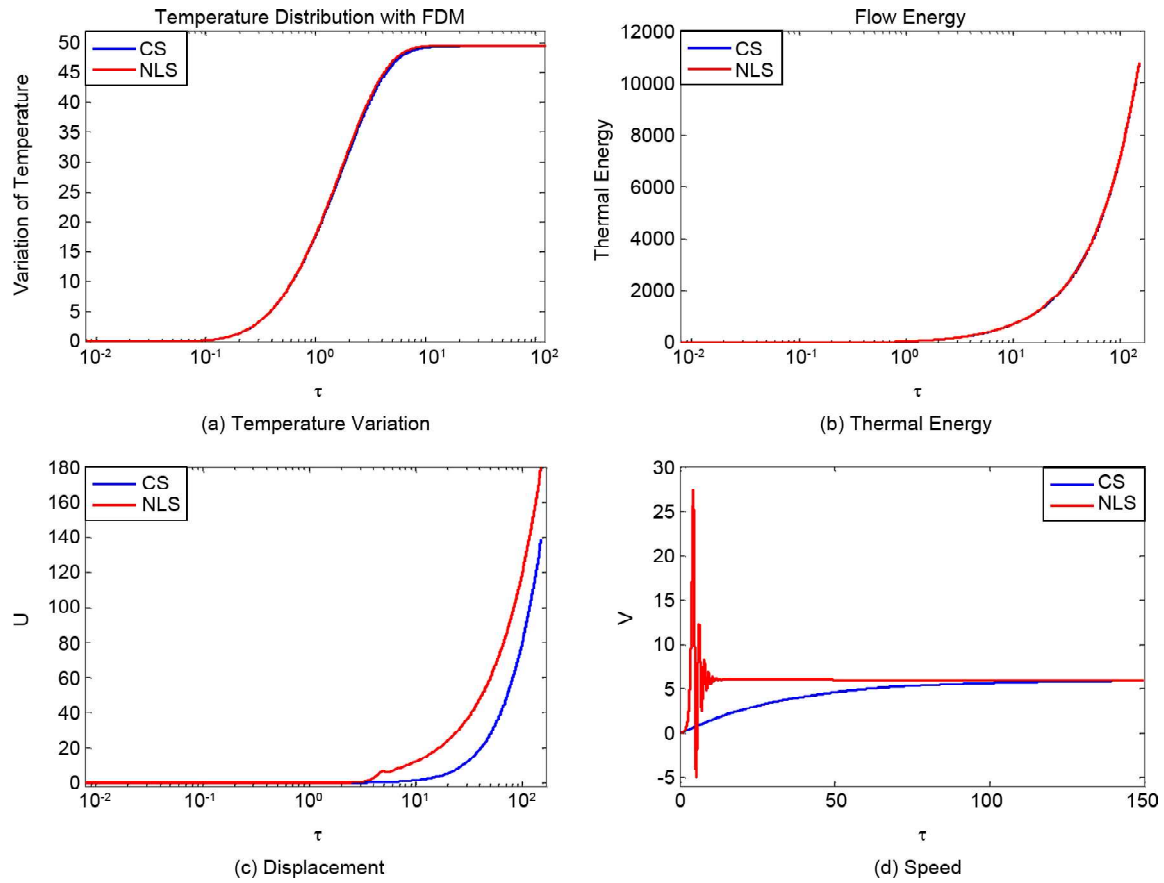

Figure 9. (a) Temperature variation, (b) thermal energy, (c) displacement, and (d) speed, for TP law for value $\eta = 7$, $U_c = 0.6$, $D_0 = 1$, $\gamma = 0$, $v = 10^{-9}$, $V_p = 0.6$, $\varepsilon_1 = 0.7$.

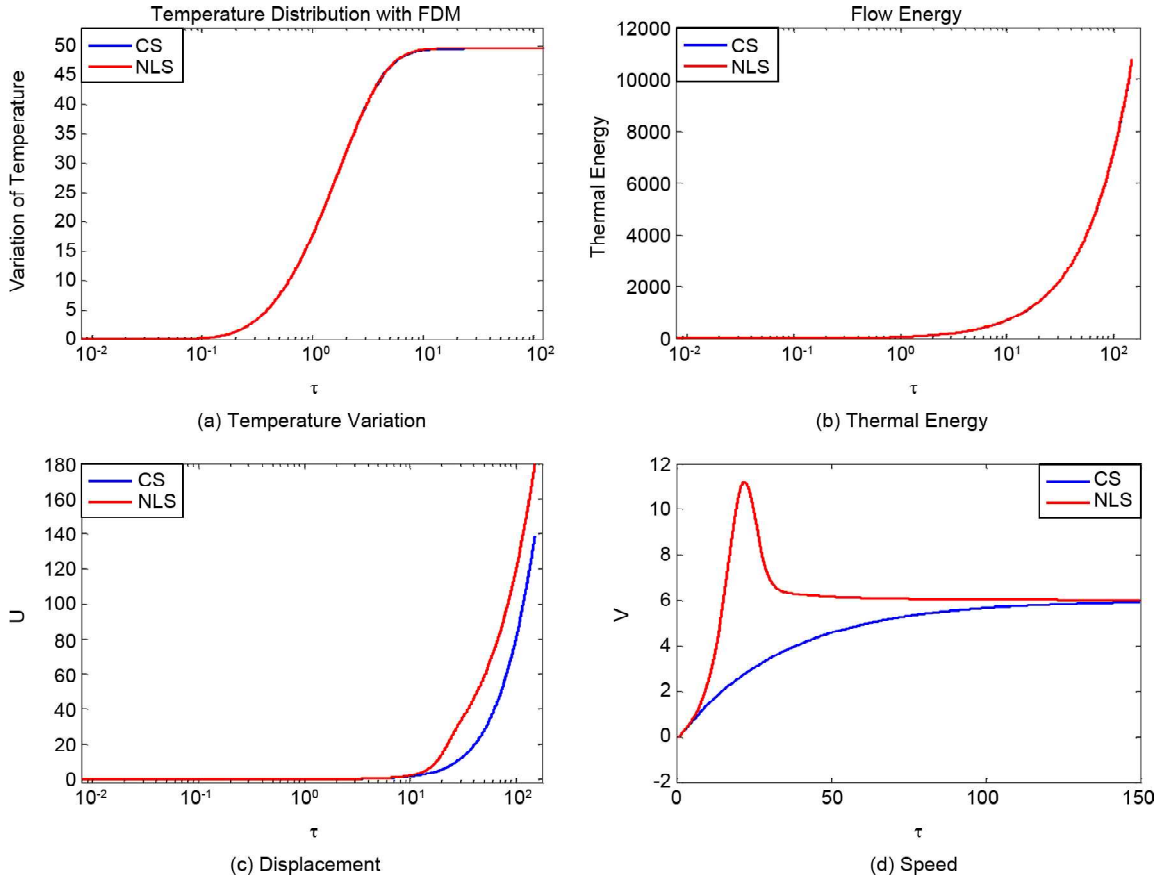

Figure 10. (a) Temperature variation, (b) thermal energy, (c) displacement, and (d) speed, for TP law for value $\eta = 7$, $U_c = 0.6$, $D_0 = 1$, $\gamma = 0$, $v = 10^{-9}$, $V_p = 0.6$, $\varepsilon_1 = 0.07$.

In absence of any internal heat source and neglecting the contributions of other energy sources at the fault level (Scholz, 1990), the energy required to set the block in motion dQ is equivalent in algebraic value to the work of frictional forces dW_F and defined by Equation (11).

$$dQ = dW_F \tag{11}$$

Now the frictional force work is by definition equal to the scalar product of frictional force by the relative speed of the block and given by the following equation:

$$dW_F = \nu F(u,\nu) \tag{12}$$

In a porous medium and in presence of a fluid, the friction force (u,ν) is proportional to both friction coefficients μ and effective stress σ^{eff} to which the mass M is subjected and is given by Equation (13).

$$\sigma^{eff} = \sigma_n - p \tag{13}$$

where, $\sigma_n = F(u,v)/S$ is normal stress to which the mass M is subjected, is the pressure of fluid flowing at fault and is the area of the pressed surface. Thus, taking into account the work of Terzaghi (1996) and Noda et al. (2009), frictional force per unit area in porous media takes the form of $f(u,\nu) = \mu\sigma^{eff} = \mu(\sigma_n - p)$. In order to reduce this relationship to an equation linking the friction to easily measurable values, we introduce here the pore-fluid ratio γ and defined by relation $\gamma = p/\sigma_n$. Thus, the frictional force per unit area in porous media becomes $f(u,\nu) = \mu(1-\gamma)\sigma_n$. When σ_n is assimilable to the force having the same dimension as the frictional force, the effective friction to which the mass M is subjected becomes:

$$f(u,\nu) = F_0\mu(1-\gamma)\exp(-u/u_c) \tag{14a}$$

In Equation (14a), F_0 is the static force and μ is a constant having the same dimension as the friction coefficient; γ and u_c are constants that represent respectively the pore-fluid ratio and a characteristic distance having the dimension of a length. Let us assume hereafter that we are $\mu_0 = \mu F_0$ positing as a constant having the dimension of the static friction, then Equation (14a) becomes the Equation (14b):

$$f(u,\nu) = \mu_0(1-\gamma)\exp(-u/u_c) \tag{14b}$$

For SH law, frictional law is written:

$$f(u,\nu) = \mu_0(1-\gamma)\exp\left(-\left(u^2 - u_c^2\right)/c^2\right) \tag{15}$$

For the SW law (Wang, 2017), frictional law is:

$$f(u,\nu) = \mu_0(1-\gamma)/(1+v/v_c) \tag{16}$$

Thus, taking into account Equations 12, 14, 15 and 16, thermal energy arising from friction at fault level in an anisotropic medium and which is necessary for the setting in motion of the block (fault rupture) is defined by Equation (17) for different frictional law:

$$dQ = Vf(U,V) = \begin{cases} \mu_0(1-\gamma)V\exp(-U/U_c) \\ \mu_0(1-\gamma)V\exp\left(-\left(U^2 - U_c^2\right)/C^2\right) \\ V\mu_0(1-\gamma)/(1+V/V_c) \end{cases} \tag{17}$$

where, U (displacement) and V (speed) are the solutions of Equations (8) (for the *TP* law), (9) (for the *SW* law) and (10) (for the *VW* law) obtained by applications of Runge's method Runge-kutta. In absence of internal heat source, the equation of heat transfer by conduction is written $\partial T^2/\partial\tau^2 = \alpha(\partial T/\partial z)$, where α is the thermal diffusivity of the surroundings. Considering the thermal energy produced by friction at the fault, the equation of heat transfer by conduction is given by:

$$\frac{\partial T^2}{\partial\tau^2} = \alpha\frac{\partial T}{\partial z} + \frac{Q(z,\tau)}{\rho c_p} \tag{18}$$

where ρ is density of the surrounding and c_p is the heat capacity of the surrounding. Equation (18) is the temperature evolution law at the level of the fault. It is coupled to the movement of the block through Equation (17).

Thus, for each of the solutions of Equations (8) (for the *TP* law), (9) (for the *SW* law) and (10) (for the *VW* law), we will evaluate the thermal energy produced by friction in the fault by the Equation (17), and we will deduce the temperature variation in the fault via the expression of Equation (18) for each friction law.

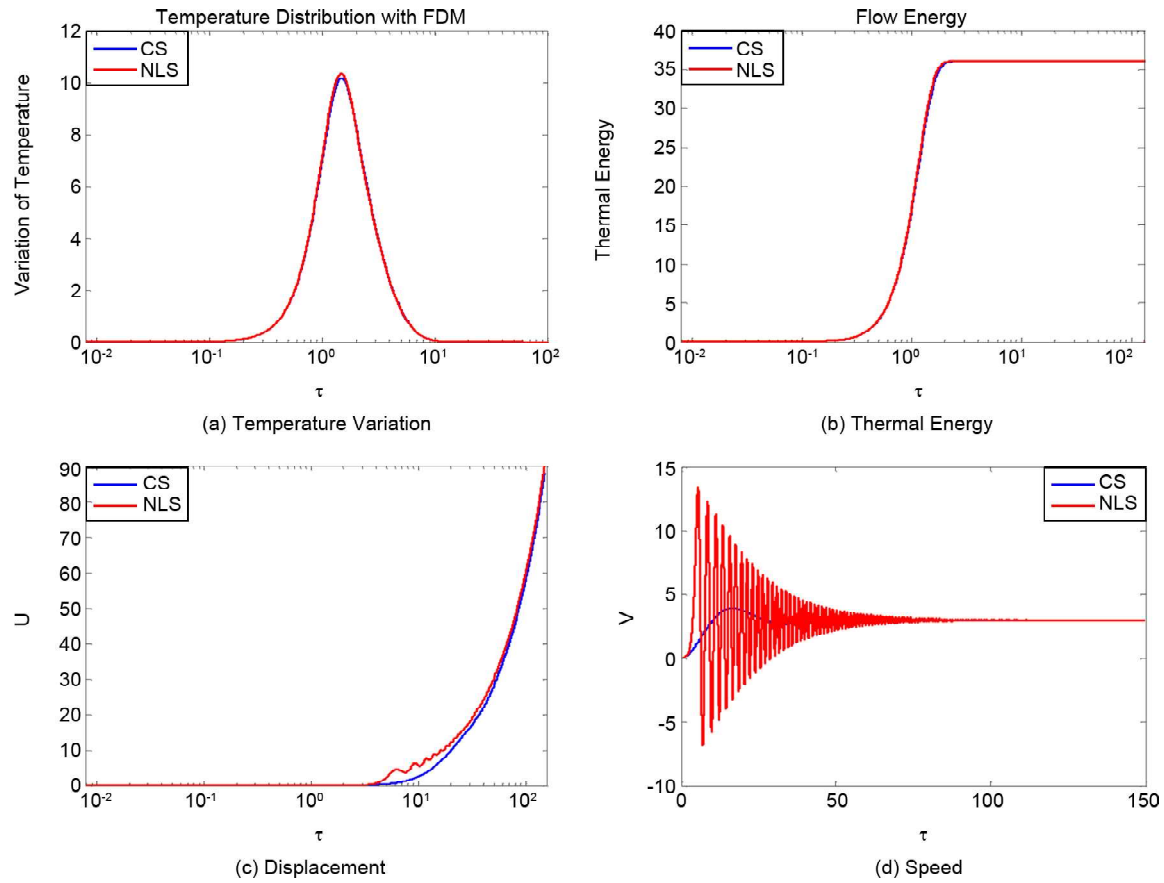

Figure 11. (a) Temperature variation, (b) thermal energy, (c) displacement, and (d) speed, for TP law for value $\eta = 0.7$, $U_c = 0.6$, $D_0 = 0.5$, $\gamma = 0.9$, $\nu = 10^{-9}$, $V_p = 0.3$, $\varepsilon_1 = 0.7$.

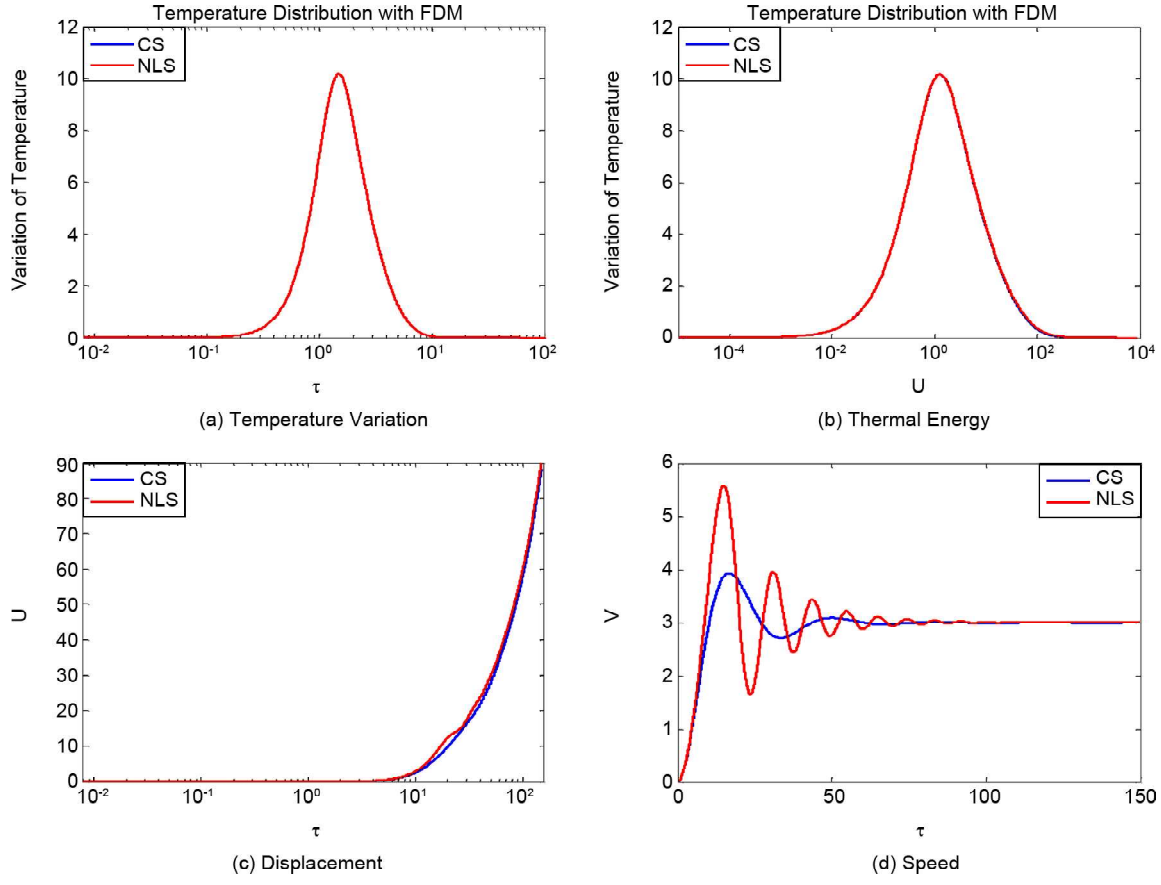

Figure 12. (a) Temperature variation, (b) thermal energy, (c) displacement, and (d) speed, for TP law for value $\eta = 0.7$, $U_c = 0.6$, $D_0 = 0.5$, $\gamma = 0.9$, $\nu = 10^{-9}$, $V_p = 0.3$, $\varepsilon_1 = 0.07$.

4. Results and Analysis

In this section, using Matlab software, we will carry out a comparative study between the case where the stiffness is constant (*CS*, red curve in Figures 2 to 12) and the case where the stiffness is non-linear (NLS, blue curve in Figures 2 to 12).

Table (1) gives the range of variation of values used during numerical representations of figures.

Numerical resolutions by the Runge-Kutta method of Equations (8), (9), (10), (17) and (18) are given by Figure (2), Figure (3) and Figure (4) for the TP law, Figure (5), Figure (6) and Figure (7) for the SH law and Figure (8), Figure (9) and Figure (10) for the VW law. For all these figures, we took $(X_0 = 0; \dot{Y}_0 = 10^{-9})$ for initial condition.

It appears from the curves that the thermal energy and the temperature variation are functions of displacement. Indeed, we observe a strong and fast increase of the thermal energy as well as the variation of temperature due to the abrupt variation of displacement during a certain time of nucleation phase until a threshold value beyond which temperature of medium also decreases abruptly tending thus towards its initial value (Figure 2a, Figure 3a, Figure 5a and Figure 6a). As for the energy curve (Figure 2b, Figure 3b, Figure 5b and Figure 6b), beyond its maximum value, energy increases and tends towards a constant limit value, which is directly proportional to the initial temperature of the surroundings. This behavior of the system can be observed both for the TP law [Figure (2a and 2b, Figure 3a and 3b)] and for the SH law [Figure (2a and 2b, Figure 3a and 3b)] when the characteristic displacements U_c and velocities of plates V_p vary. As for the VW law [Figure (8a and 8b), Figure (9a and 9b)], we observe a sudden increase in thermal energy and temperature as a function of displacement; the temperature increases up to a threshold value and then stabilizes tending towards a constant value different from the initial value.

Energy increases up to a fixed limit value which is proportional to the displacement. Comparing the curves obtained when the stiffness is non-linear (NLS, red line) and when the stiffness is constant (CS, blue line), although a qualitative difference in the temperature and heat profiles is not observable when passing from one law to another, a quantitative difference is noted when the parameters of the system change.

For large values of U_c and V_p simultaneously and for $0.1 \prec \varepsilon_1 \prec 1$, is noted a multitude of oscillations in the velocity profile and those in an extremely short interval of time before stabilization towards a fixed value, both for the TP (Figure 2c, Figure 3c), SH (Figure 5c, Figure 6c) and VW (Figure 8c, Figure 9c) law. In the case where $\varepsilon_1 \prec 0.1$ (Figure 4c for the TP law, Figure 7c for the SH law and Figure 10c), the speed increases very quickly to reach its maximum value after decreases towards a constant fixed value close to the one obtained when the elasticity coefficient is assumed to be only constant. We can deduce that for very low values of $\varepsilon_1 (\varepsilon_1 \prec 0.1)$, the system grows and

Table 1. Range of variation of parameters used during figure plotting.

	η	U_c	D_0	γ	ν	V_p	ε_1	ε_2	ε_3
Figure 2	7	0.6	0.5	0	10^{-9}	0.3	0.7	0	0
Figure 3	7	0.9	1	0	10^{-9}	0.6	0.7	0	0
Figure 4	7	0.9	1	0	10^{-9}	0.6	0.07	0	0
Figure 5	7	0.6	0.5	0	10^{-9}	0.3	0.7	0	0
Figure 6	7	0.9	1	0	10^{-9}	0.6	0.7	0	0
Figure 7	7	0.9	1	0	10^{-9}	0.6	0.07	0	0
Figure 8	7	0.6	0.5	0	10^{-9}	0.3	0.7	0	0
Figure 9	7	0.9	1	0	10^{-9}	0.6	0.7	0	0
Figure 10	7	0.9	1	0	10^{-9}	0.6	0.07	0	0
Figure 11	0.7	0.6	0.5	0.9	10^{-9}	0.3	0.7	0	0
Figure 12	0.7	0.6	0.5	0.9	10^{-9}	0.3	0.07	0	0
Figure 13	7	0.9	0.55	0.9	10^{-9}	0.3	0.7	0.5	0.3
Figure 14	7	0.9	1.63	0.9	10^{-9}	0.6	0.07	0.05	0.03
Figure 15	7	0.9	1.63	0.6	10^{-9}	0.6	0.3	0.09	0.03

converges towards a state of stable equilibrium, contrary to the case where $0.1 \prec \varepsilon_1 \prec 1$.

By comparing Figures (2) and (3) (TP law), and Figures (4) and (5) (SH law), we can clearly see that temperature and thermal energy produced by friction increase with the increase of the value of U_c and V_p for zero values of the lubrication coefficient.

However, when the value of lubrication coefficient increases, the values of thermal energy and temperature produced by friction decrease with time. As for the VW law, we notice that any variation of U_c and V_p does not affect the amplitude or the dynamics of the evolu-tion system, which is justified by the fact that the system does not depend on U_c.

Comparing the curves of the temperature variation obtained for the NLS with CS, it noted that although the curves have the same profiles, amplitude where the amount of energy produced by friction NLS is greater than the one of energy produced by the CS, thus highlighting the importance of the CS (see Figures 2 to 12).

This conformity in the temperature and energy profiles is justify either by the structure of the fault and the shape of the contacts that prevail there, or by the definition of the thermal energy that is only proportional to the variation of velocity of the block and to the friction, which are two quantities that do not depend directly on the elasticity coefficient.

5. Study Cases for $f \neq 0$

Previous figures have been obtained assuming that pore-fluid ratio is zero ($\gamma = 0$). Figures (2) to (12) allow saying that the dynamics of the system remains almost constant when passing from one friction law to another. This implies that the consideration of anisotropy in this study has the effect of stabilization of the system whether passing from one law of friction to another. In what follow, we will only focus on the TP law, because it better converge than the others according to this study.

In the analysis now, let admit that the surrounding is porous, with p the pressure of the fluid circulating at the walls.

Therefore, the lubrication coefficient γ becomes a non-zero constant. This is equivalent to the cases where the friction law is defined by Equation (14) and the system of Equation (8) takes the form of Equation (19).

Many works (Konga et al., 2017, 2020; Wang, 2017; Dongmo, et al. 2014) have studied the dynamics of such system when the parameters such as viscosity (Konga et al., 2020), friction coefficient (Konga et al., 2017), lubrication coefficient (Dongmo et al., 2014) or characteristic displacement (Wang, 2017) varied.

That's why in the following, we will be holding all other values constant and then evaluated the behavior of the system at different ε_1 value in order to understand the contribution of nonlinearity of the elasticity coefficient in the dynamics of the system.

$$\begin{cases} \dfrac{dX}{d\tau} = Y \\ \dfrac{dY}{d\tau} = -\left[1-\varepsilon_1^2 D_0 V_p \tau\right] X - \eta Y - \ldots \\ \quad \mu_0 (1-\gamma) \exp\left(-\dfrac{X}{U_c}\right) + V_p \tau - \varepsilon_1^2 D_0 X^2 \end{cases} \tag{19}$$

Numerical solutions of Equation (19) are given in Figure (11) and Figure (12). Note that the cases where the stiffness is constant (CS) are represented by the curves in blue, and the cases where the stiffness is nonlinear (NLS) are represented in red.

Figure (11) and Figure (12) show that in the presence of non-linearity and when pore-fluid ratio $\gamma \neq 0$, the system increases abruptly to a threshold value, then decreases while oscillating with a multitude of decreasing amplitudes and according to a certain envelope for large value of the frequency ε_1 (Figure 11).

The decrement is perpetuated over time to finally reach to a stable value equivalent to those obtained when the stiffness is constant. For constant values of the parameters of the system used, we notice that the number of oscillations of the system decreases when the parameter decreases (Figure 12).

This is justified in reality by the fact that decreasing of ε_1 assumes that the seismic wave during nucleation phase has propagated in

refractive media (with low stiffness) to a more refractive medium (with high stiffness), where the seismic wave has difficulty in propagating and the signal tends more quickly to its stable value.

For values of $0 \prec \gamma \prec 1$, the more the value of γ is larger and closer to unity, the more the amplitudes of the signals decrease with time. As the value of γ decreases tending to zero, the signal amplitudes increase closely to its maximum value.

Thus, the effect of the porosity of the fault as well as the presence of a fluid has the effect of decreasing the intensity and the amplitude of the signal. In general, the amplitude of signal decreases with increasing value of pore-fluid ratio γ.

The introduction of anisotropy in the stiffness reveals in the speed profile the existence during the nucleation phase of a loading zone (stick) of decreasing amplitude for the TP, SH and VW laws characteristic of the change in property of the medium. By observing the speed profiles for the same parameters when the stiffness is constant, we see that this loading zone does not exist. In the displacement profile, it highlights a change in the concavity zone of the curve that is not observed when the stiffness is constant. The non-linearity of the stiffness also reveals in the speed profiles the existence of a transient phase, characterized by oscillations of decreasing amplitude in time before steady state.

6. Other Study Cases

Let us now return to initial Equation (3) by considering the third-order nonlinearity, and let set $\varepsilon_1 = \omega_1/\omega_0$, $\varepsilon_2 = \omega_2/\omega_0$ and $\varepsilon_3 = \omega_3/\omega_0$ then Eq-uation (6) without simplification and without approximation becomes:

$$\frac{d^2U}{d\tau^2} = -\left[1 + \varepsilon_1^2 D_0 U + \varepsilon_2^2 D_0^2 U^2 + \varepsilon_3^2 D_0^3 U^3\right]U - \eta\frac{dU}{d\tau} - \mu_0(1-\gamma)\exp\left(-\frac{U}{U_c}\right) + \left[1 + \varepsilon_1^2 D_0 U + \varepsilon_2^2 D_0^2 U^2 + \varepsilon_3^2 D_0^3 U^3\right]V_p\tau \quad (20)$$

By analogy with the fourth-order Runge-Kutta solution that we have already stated in section (3 and 4) to solve our differential equations, Equation (20) becomes:

$$\begin{cases} \dfrac{dX}{d\tau} = Y \\ \dfrac{dY}{d\tau} = -\left[1 + \varepsilon_1^2 D_0 X + \varepsilon_2^2 D_0^2 X^2 + \varepsilon_3^2 D_0^3 X^3\right]X - \\ \eta\dfrac{dX}{d\tau} - \mu_0(1-\gamma)\exp\left(-\dfrac{X}{U_c}\right) + \\ \left[1 + \varepsilon_1^2 D_0 X + \varepsilon_2^2 D_0^2 X^2 + \varepsilon_3^2 D_0^3 X^3\right]V_p\tau \end{cases} \quad (21)$$

Numerical solution of Equation (21) for different value of ε_1, ε_2 and ε_3 are given by Figures (13) to (15).

For higher-order nonlinearities, as $\varepsilon_i \prec 1$ with i = 1, 2, ... in Figure (13), the system vibrates with increasingly increasing amplitudes up to a threshold value beyond which the amplitudes decrease to a state of balance. Each amplitude peak is separated from the previous one by a different transient phase close to zero. The evolution profile of temperature versus time and energy versus time reveals that they are substantially the same when going from first-order nonlinearity to higher-order nonlinearity. This is because we used a flaw of thickness 2w in our representations. For $(\omega_i/\omega_0)^2 \prec\prec \varepsilon_1$ with $i \succ 2$, the system is most stable when we move to the higher order nonlinearity ($i \succ 2$) (see Figure 15).

The numerical analysis of our system reveals that when $(\omega_i/\omega_0)^2 \succ 1$, the system is unstable and any perturbation of their intrinsic parameters leads to a large variation of behavior of the system. We can therefore deduce in this interval of variation of the pulsation, the quasi-chaotic system.

For $\forall\, i \succ 2$, when $(\omega_i/\omega_0)^2 \prec (\omega_1/\omega_0)^2$ and $(\omega_i/\omega_0)^2 \prec\prec\prec (\omega_1/\omega_0)^2$ (see Figures 13 to 15), the system is quasi-static such that any perturbation in the system almost leads to a stable state. Thus, for nonlinearities of order greater than three, the study system admits a steady state for very small values of pulsations of order greater than two.

When $\varepsilon_1 \prec\prec 1$ and the pore-fluid ratio is non-zero ($\gamma \neq 0$), i.e., when the stiffness of the middle in which the seismic wave originates is lower than those of the middle in which the wave propagates. Hence the difference between the wave that propagates when the stiffness is constant (CS) and the anisotropy case (NLS) is not very visible (for first-order nonlinearity) to the point where everything happens as if in both cases, the seismic wave

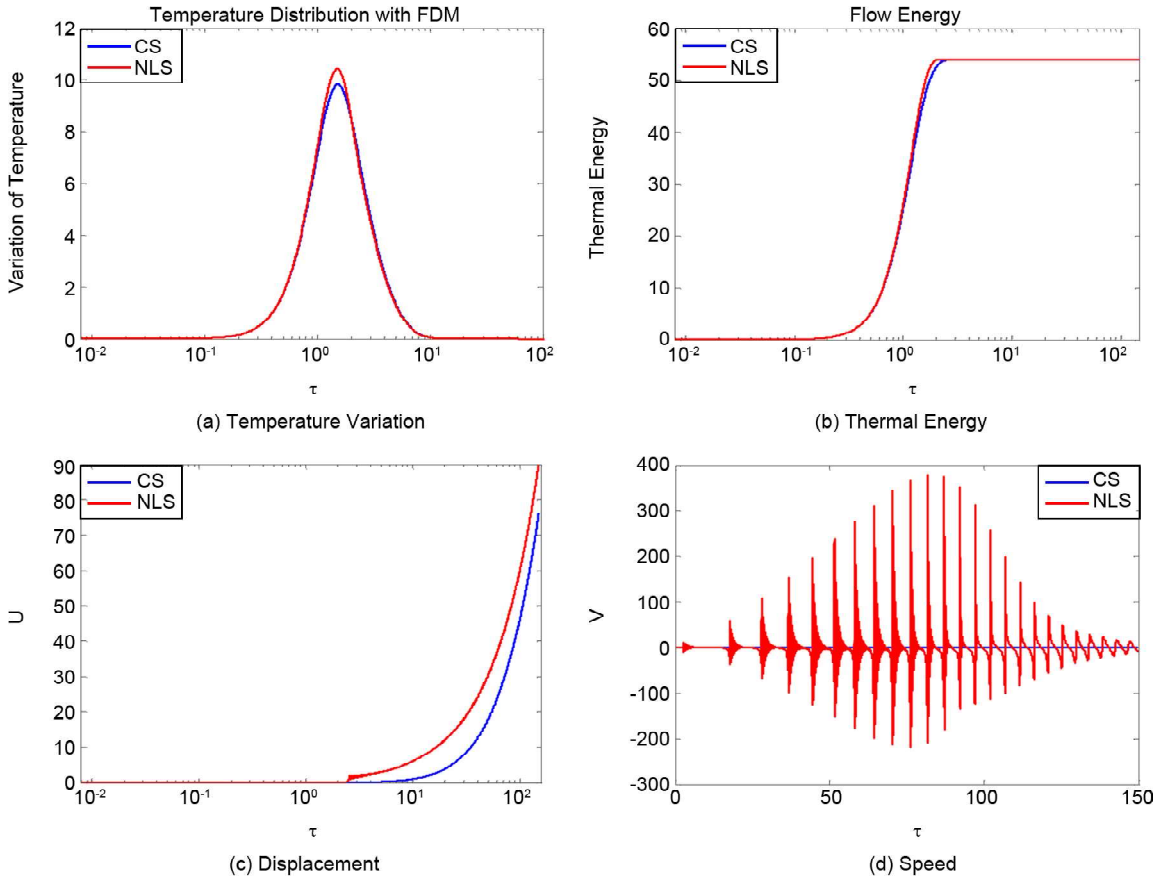

Figure 13. (a) Temperature variation, (b) thermal energy, (c) displacement, and (d) speed, for TP law for value $\varepsilon_1 = 0.7$, $\varepsilon_2 = 0.5$, $\varepsilon_3 = 0.3$, $\eta = 7$, $U_c = 0.9$, $D_0 = 0.55$, $\gamma = 0.9$, $v = 10^{-9}$, $V_p = 0.3$.

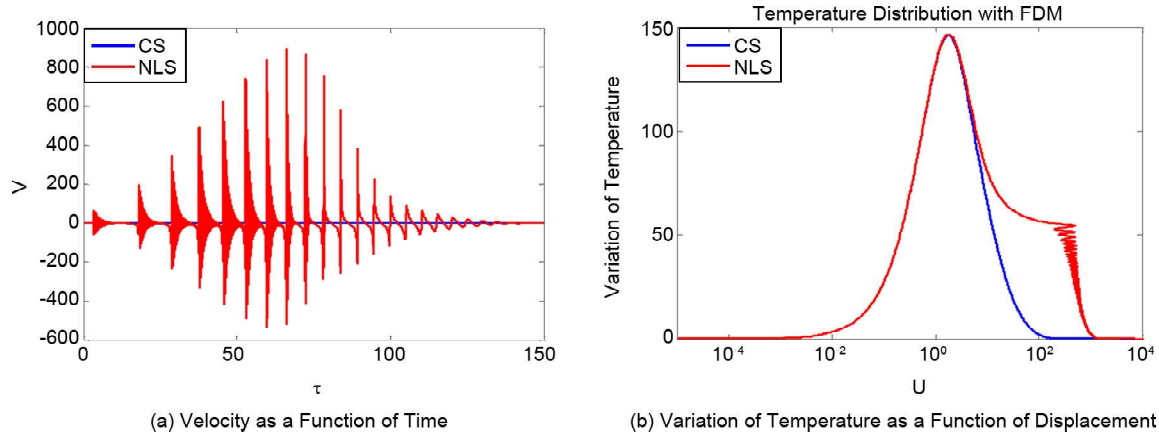

Figure 14. Third-order plot of, (a) velocity as a function of time, (b) variation of temperature as a function of displacement, for $\varepsilon_1 = 0.07$, $\varepsilon_2 = 0.05$, $\varepsilon_3 = 0.03$, $\eta = 7$, $U_c = 0.9$, $D_0 = 1.63$, $\gamma = 0$, $v = 10^{-9}$, $V_p = 0.6$.

is reduced to a wave that propagates in phase shift (see Figure 12).

Indeed, by observing the evolution profiles of the velocity, it can be seen that they grow rapidly in time until a maximum value beyond which the curve abruptly changes the concavity before continuing its progression but with a steeper slope than the previous ones.

The case when $\omega_i = cste$ $(k_i = cste = k_0)$, show that a seismic wave propagates in an isotopic middle; the system grows botfly in time and space exponentially and strongly while maintaining its dynamics. However, for $\omega_i \neq cste$ (where $\omega_0 \neq \omega_1 \neq \omega_2 \neq \omega_3 \neq ....$) and $(\omega_i / \omega_0)^2 \prec 1$, the amplitudes of the system grow in time with an effect of modifying the dynamics of the system when the intrinsic parameters of a system change.

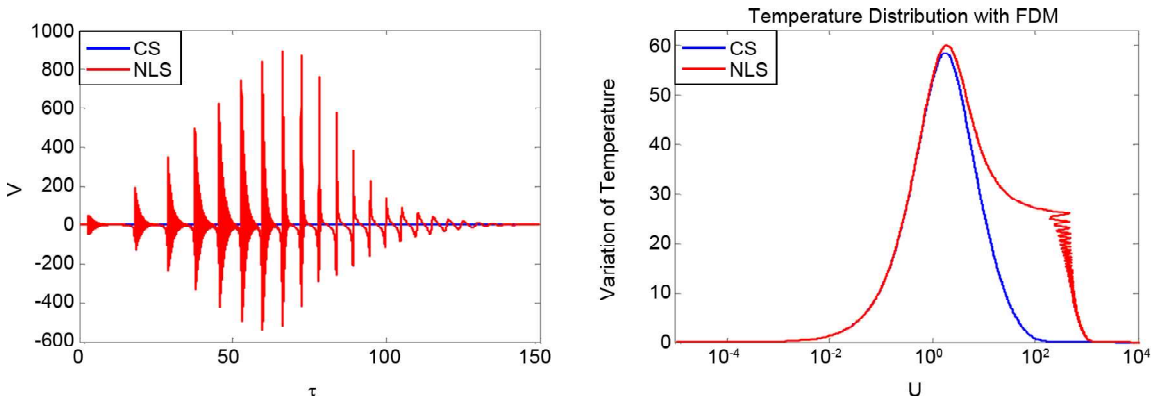

(a) Velocity as a Function of Time (b) Variation of Temperature as a Function of Displacement

Figure 15. Third-order plot of, (a) velocity as a function of time, (b) variation of temperature as a function of displacement, for $\varepsilon_1 = 0.3$, $\varepsilon_2 = 0.09$, $\varepsilon_3 = 0.03$ and for $\eta = 7$, $U_c = 0.9$, $D_0 = 1.63$, $\gamma = 0.6$, $v = 10^{-9}$, $V_p = 0.3$.

7. Discussion

In this work, we studied the effect of non-linearity of stiffness (NLS) on the dynamics of nucleation of an earthquake. For this purpose, we started with a 1D model of an earthquake (Burridge-Knopoff model) to generate the second-degree differential equation with a non-constant coefficient translating the dynamics of a system (for first-order nonlinearity and for higher order nonlinearity). Since analytical resolution of these equations is not easy by conventional methods, a numerical approach was established in order to provide solutions of our system. The numerical resolution of this equation being based on the four order Runge-Kutta algorithm allowed us to obtain the dimensioned profiles of displacement, velocity and energy produced by friction (necessary to produce the rupture) at the level of the fault for different form of the friction function. Then we compared the results obtained when the stiffness is constant (CS) and when the stiffness is non-linear (NLS). It was found that:

When stiffness varies, the stick-slip phenomenon is highlighted during nucleation phase. Both for first-order nonlinearities and for higher-order nonlinearities. This behavior of the system is much more visible for higher-order nonlinearities, as illustrated in Figures (13) to (15). Indeed, for nonlinearities of order one (Figures 2 to 12), the dynamics of our system shows that the dependence of the stiffness on space (NLS), reveals in a first phase a great increase of the speed of slip of your system, which falls again immediately and those in an interval of time extremely short, then the phenomenon starts again (in a movement of oscillatory peak) with amplitudes increasingly small until cancellation of the oscillations. This sudden variation of the oscillations of the system corresponds to the stick. In another phase, after the cancellation of the oscillations in the previous phase, the dynamics of our system stabilizes and tends towards a fixed value of the speed, which is perfectly quantifiable (steady-state). This second phase corresponds to the sliding phase; however, for higher-order nonlinearities (Figures 13 to 15), the same behavior is observed, which is repeated successively with increasing amplitudes up to a threshold value beyond which it decreases symmetrically towards a value close to the initial value. This result is in agreement with the literature and can be observed both for the TP, SH and VW law. Indeed, on the basis of experimental work carried out in laboratory and theoretical modeling, authors such as Dieterich (1979, 1992), Ohnaka et al. (1987), Andrews (1976), Brune (1979), and Das and Scholz (1981) have revealed the existence of a small and then steady-state slip phase before (nucleation phase) any large seismic rupture at the fault. Other works such as Gomberg and Davis (1996), Brodsky et al. (2000), Gomberg and Reasenberg (2001) had also suggested the existence of a small event preceding the crossing of seismic wave. Putting together these two phases highlights the stick-slip motion. Whereas for the same values of the parameters of the system with constant stiffness, the dynamics of the system reveals that relative slip velocity of our system simply increases with time, tending towards the

same limit value as the one observed when the stiffness is non-linear. More generally, when comparing the velocity profiles obtained for $\gamma \neq 0$ and $\gamma = 0$ when the stiffness is non-linear (NLS), we notice a multitude of oscillations corresponding in reality to the multitude of microseisms with increasing amplitude (which are related to heterogeneity) that are recorded at regular intervals of time during nucleation phases. Indeed, Nur (1978) showed that the resistive stress would tend to become uniform with/after successive earthquakes until all events rupture the entire fault length and processes cease to become important.

In the absence of non-linearity (CS), the nucleation time decrease. We notice that, the velocity grows rapidly and leads directly to its steady state value. While considering the non-linearity of the stiffness (NLS), we clearly observe that the nucleation time during which the seismic wave grows very weakly until a maximum value (limit) and then start to decrease strongly while converging to another steady value different from the initial value, showing therefore the existence of a transient phase before any stable state during the nucleation phase. We can also conclude that after a certain excitation, the system goes from an initial steady state to another different from the previous one, which correspond to the transitory phase existing before any great earthquake. This behavior of the system is perfectly demonstrated for higher-order nonlinearities. Such an accumulation of the effects of the previous seismic activities clearly explains the memory effect of an earthquake. Moreover, accumulation of the memories of different seismic excitations will push the system to its elastic limit, beyond which the system will fail causing earthquake itself. Some previous works as those of Scholz et al. (1972), Dieterich (1981), Ohnaka and Yamashita (1989), Kato et al. (1994), and Roy and Marone (1996) have also shown the existence of this transient phase in the nucleation process preceding any great earthquake.

The comparative analysis of the evolution curves of the velocity as a function of time reveals that, for the non-linearity of order one, the system represented is only an isolated state of the system.

However, for higher-order non-linearities (Figures 13 to 15), our system highlights the various microseismic activities of increasingly increasing amplitudes that are observed during the nucleation phase of an earthquake. The phenomenon repeats itself up to a speed of maximum amplitude, beyond which the amplitude decreases until it cancels out. Thus highlighting the symmetry of the phenomenon. This symmetry of our system turns out to be an asset to justify the aftershocks observed during seismic events. By admitting the non-linearities of order one, we have generally observed a stability in the evolution of the system when we pass from one value to another on the one hand, and when we pass from a law of evolution of friction to another. However, this stability of the system is no longer verified when we move on to higher-order nonlinearities.

The temperature evolution curves for the TP law and for the VW law reveal that they evolve according to a normal law. This assumes that all the heat produced by friction at the fault is dissipated around the fault. This shape of the temperature profiles can justify the choice of a binomial law (giving the evolution of temperature as a function of time and space) as a mathematical model to represent the temperature that certain authors have made (e.g., Fialko, 2004). As for the temperature profile for the VW law, it reveals the existence of a temperature distribution function of space and time, reflecting its evolution. This result for the VW law is valid for both the NLS and the CS. For some values of the system parameters and in some intervals of time, the speed is negative (e.g., Figure 2d). It means that at these intervals, the polarity of the movement has changed (polarity change is due to the stick-slip movement). Therefore, the direction of the slip and the direction of the force remain in opposition.

The introduction of the spatial variation of stiffness in the system proved in advance the importance of heterogeneity during the nucleation phase of an earthquake. Indeed, Schar et al. (2021) already pointed out that the nucleation process is particularly important because it determines the stress level at which the frictional interface fails, and therefore, the macroscopic friction strength. This is what can be seen in

Figures (13) to (15) for hygher-order of non-linearities. There are also crepe-to-crepe oscillations characteristic of the different asperities observed along a fault. To this end, Cattania and Segall (2021) thought that the pre-seismic phase is characterized by feedback between creep and foreshocks, i.e., during the pre-seismic phase, we observe episodic seismic bursts breaking groups of nearby asperities, causing creep to accelerate, which in turn loads other asperities, leading to further foreshocks.

The results of this work show that whatever the values of the surrounding parameters of our model, the temperature profiles remain substantially the same for both the TP law and the SH law for first-order of non-linearities. In general, it is observed that the amplitude of the signal grows when the value of the characteristic distance increase. Moreover, a comparative study between the case where the stiffness is constant and variable (anisotropy) reveals that the existing load time before any seismic activity is reduced, and the displacement profile show the non-uniformity in the wave propagation characteristic of an inhomogeneous Earth's crust in accordance with the Motchongom et al. (2022) conclusion.

By comparing the profiles of the temperature variation curves for the TP, SH, and VW laws, we deduce that the TP and SH seem more stable than the VW law. Indeed, according to their temperature variation profiles, we observe a symmetry and convergence of temperature values in a very fixed time interval despite variations in the system parameters. This symmetry is justified by the form of the Gaussian friction functions for the TP and the SH laws. Indeed, the analysis of the friction functions for the TP and SH laws reveals that these two functions remain stable for any variation of U_c (TP law) and C (SH law), respectively, included in a very precise interval, and beyond this interval, the function is null. Thus, any variation in the behavior of the system or any external stress imposed on the system in this interval has the effect of always returning the temperature to its original point during the nucleation phase; hence, its variation is zero for the TP and the HS laws. On the other hand, for the VW law, we note that any variation in the behavior of the system or any external stress has the effect of causing the temperature to pass from an initial stable state to another state, although stable but different from the initial state. From this convergence of the temperature over a very precise time interval and taking into account the non-linearity of the stiffness, we can deduce that during the nucleation phase, there exists a time interval for which the stick-phenomenon slip occurs. This behavior of the system is confirmed by the speed evolution curves, on which we immediately observe a damped oscillatory movement followed by a constant phase translated by a uniform movement at constant speed. Thus, the non-linearity of the stiffness highlights the seismic micro-activities as well as the heat production during the nucleation phase, highlighting the importance of the non-linearity of the stiffness during the nucleation phase in the dynamics of an earthquake. This is also what Harris et al. (2021) revealed when they talked about the importance of heterogeneity in the nucleation process of an earthquake.

By comparing the evolution curves of the thermal energy produced by friction for the TP, SH, and VW laws, we see that analogously to that of the temperature variations for the TP, SH and VW laws, the energy profile reveals that for any external stress on the system in its nucleation phase, the system passes from an initial stable state to another final stable state for the TP and SH laws, whereas for the VW laws, the system is constantly evolving. These analyses of the system support our point of view that the TP and SH laws are more stable than the VW laws during the nucleation phase.

When $\gamma \neq 0$, it can be seen that the system is sensitive to variations in ω_i, which are quantities directly linked to the stiffness k_i and which correspond to the different degrees of non-linearity. This proves that the introduction of nonlinearity induces that the system is dependent on the elastic properties of the medium. Harris et al. (2021) already obtained the same conclusion during their work on Geology and Geodesy Based Model of Dynamic Earthquake Rupture on the Rodgers Creek-Hayward-Calaveras Fault System, California. Such concordance between this work and the one of literature rightly justifies the quality of the model

adopt to produce such result.

For $\gamma \neq 0$, i.e., assuming that the porous rock with a fluid circulating therein, a decrease in the amplitude of the seismic displacement as well as in the sliding velocity is observed, which has the direct effect of reducing the stress exerted on the rock and therefore reduce the loading time of an earthquake. This result emphasizes the importance of thermal pressurization of rocks in the fault nucleation process as also shown by Mase and Smith (1987). The linear variations observed in the velocity and displacement profiles for $\gamma = 0$ and $\gamma \neq 0$ can be due either to the discontinuities encountered in the Earth crust, or to the structure of the fault (asperity, geometry) or even to the thermal pressurization of the medium. Indeed, in their work on the dynamics of the fault of San Andrea, Lachenbruch and Sass (1980), Lachenbruch (1980) showed that the existence of anomalies in the structure of the fault was due to the dynamic friction in the fault caused by the thermal pressurization. Some authors (Sibson, 1973; Lachenbruch, 1980; Holcomb, 1981; Mase & Smith, 1987) approves that the recovery of dilatency accompanying the release of shear stress during faulting can cause a negative pore dilation and therefore a further improvement in the rate of thermal pressurization, which could also justify its variations.

The decrease in velocity as a function of time in the model is comparable to the decrease in the coefficient of friction over time or as a function of characteristic slip in some works (Wang, 2017). During seismic sliding, the coefficient of friction passes from its dynamic value (which is inversely proportional to the characteristic displacement) towards a stable and constant value. This behavior of the coefficient of friction is highlighted in the velocity and temperature profiles plotted, in which it clearly observes a decrement and a convergence towards a fixed value. These observation results are valid for the NLS (nonlinear stiffness) as for the CS (constant stiffness).

8. Conclusions

In this article, it was a question for us to study the effect of spatial variation of the stiffness (anisotropy surrounding) during the nucleation phase of an earthquake. For this, we considered a one-dimensional model of Burridge and Knopoff studied by Wang (2017), in which we introduced a linear (spatial) variation of the stiffness in order to determine the displacements, velocities, thermal energies and variation of the temperature for different expressions of friction laws (for the TP law, SH law and VW law). In this work, we have not discussed the sign and the magnitudes of the stiffness after its limited development. Because the model is a harmonic vibrating system subjected to an external exciting source, it can operate either in compression (for the values of negative k) or in tension (for the values of positive k).

By introducing the non-linearity in the stiffness and by comparing the curves obtained as well for the TP law, the SH law as well as for the SW law, it was concluded that the non-linearity of the stiffness (NLS) had for effect of stabilizing the system when passing from one law to another. Moreover, by comparing the cases where the stiffness was constant (CS) and the cases where the stiffness varied in space (NLS), we concluded that the introduction of nonlinearity generated during the nucleation phase a stick-slip phenomenon.

This study highlighted the importance of non-linearity in the nucleation process. Indeed, we showed that in order to evaluate the microseisms recorded during the nucleation phase, the introduction of non-linearity in the stiffness was also important. Each microseism is separated from the next by a coseismic phase (transient phase). The introduction of nonlinearity in the stiffness revealed the presence of a multitude of microseisms having successively decreasing amplitudes over time during the nucleation phase. Assuming that the stiffness was not constant, we showed that the loading time during the nucleation phase decreased and that there was a transitional phase between the different seismic elements.

The comparative study that was carried out on the different friction laws showed that the VW was much more unstable than the TP law and SH law. We have shown that there exists a time interval for which the TP law and SH law converge and evolve following a Gaussian, and beyond this interval, any variation in the system parameters is zero.

In the presence of the pore-fluid ratio, that is, for the pore-fluid ratio different from zero and for nonlinearities of order one and greater than one, we have shown that the fluid has the effect of reducing the amplitude of the signal while retaining the shape of the initial profile obtained when the pore-fluid ratio is zero.

We have established a correlation between the behavior of our system and the evolution of the coefficient of friction during its evolution, observed in other works. The compliance of our work with certain suggestions and theories expressed in the work of our predecessors led us to conclude that our model can be integrated into existing seismic prediction models. Because the 1D model is a simplified representation of the earthquake, we intend to adapt it to a multidimensional coupled dynamics of an earthquake during its nucleation phase in order to see how it contributes to a structure close to the fault geometry in our next work.

9. Declarations

- Ethics Approval and Consent to Participate

The authors all approve and consent to participate

- Consent for Publication

The manuscript titled: "Effect of non-linearity of stiffness during the nucleation phase of an earthquake", proposed by Djiogang Francis Olivier, Koumetio Fidèle and Yemele David is not subject to any conflict of interest and may be published in the review JSEE in case of acceptance. The authors all consent to this publication.

- Availability of Data and Material

Not applicable

- Competing Interests

The authors declare that the manuscript entitled "Effect of non-linearity of stiffness during the nucleation phase of an earthquake" has never been published partially or totally elsewhere and is not subject to any conflict of interest.

- Funding

Not applicable

- Authors' Contributions

This manuscript entitled "Effect of non-linearity of stiffness during the nucleation phase of an earthquake" was thought out, put into equation and written by DJIOGANG Francis Olivier. The complexity and non-linearity of the equations forced us to adopt a numerical approach. This method of resolution was carried out by DJIOGANG Francis Olivier and KOUMETIO Fidèle, and under the supervision of YEMELE David. Proofreading and verification are carried out by KOUMETIO Fidèle and YEMELE David. The discussion and validation of the manuscript was jointly done by Djiogang Francis Olivier, Koumetio Fidèle and Yemele David.

Acknowledgements

We would like to thank the editor-in-chief and his entire team for agreeing to publish our article in his journal. We thank the various reviewers whose criticisms and comments have improved the quality of the manuscript. We would like to thank the entire research team who greatly contributed to the production of this article.

Article Highlights

This article studies and solves the effect of the non-linearity of the stiffness during the nucleation phase of an earthquake. The output show that in such case, the stick-slip movement takes place; the system tends towards steady state for different law of friction and that there always exists a transitory phase before this steady state. Also proved in this work, the existence of a multitude of micro events with decreasing amplitudes during the nucleation phase.

References

Ampuero, J.-P., Ripperger, J., & Mai, P.M. (2006). Earthquakes: Radiated energy and the physics of faulting. *American Geophysical Union (AGU)*, 255-261.

Andrews, D.J. (1976). Rupture velocity of plane strain shear cracks. *Journal of Geophysical Research*, *81*(26), 5679-5687.

Burridge, R., & Knopoff, L. (1967). Model and theoretical seismicity. *Bulletin of the Seismological Society of America*, *57*(3), 341-371.

Brodsky, E.E., Karakostas, V., & Kanamori, H.

(2000). A new observation of dynamically triggered regional seismicity: Earthquakes in Greece following the August 1999 Izmit, Turkey earthquake. *Geophysical Research Letters*, 27(17), 2741-2744.

Brune, J. (1979). Implications of earthquake triggering and rupture propagation for earthquake prediction based on premonitory phenomena. *Journal of Geophysical Research*, *84*(B5), 2195-2198.

Cao, T., & Aki, K. (1984). Seismicity simulation with a mass-spring model and a displacement hardening-softening friction law. *Pure and Applied Geophysics*, *122*(1-2), 10-24.

Cao, T., & Aki, K. (1986). Seismicity simulation with a rate and state dependent friction law. *Pure and Applied Geophysics*, *124*(4-5), 487-513.

Carlson, J.M., & Langer, J.S. (1989). Mechanical model of an earthquake fault. *Physical Review A*, *40*(11), 6412-6424.

Cattania, C., & Segall, P. (2021). Precursory slow slip and foreshocks on rough faults. *Journal of Geophysical Research: Solid Earth*, 126(e2020JB020430).

Das, S., & Scholz, C.H. (1981). Theory of time-dependent rupture in the earth. *Journal of Geophysical Research*, *86*(B7), 6039-6057.

Di Toro, G., Pennacchioni, G., & Teza, G. (2005). Can pseudotachylytes be used to infer earthquake source parameters? An example of limitations in the study of exhumed faults. *Tectonophysics*, *402*(1-2), 3-20.

Dieterich, J.H. (1979). Modeling of rock friction 1. Experimental results and constitutive equations. *Journal of Geophysical Research*, *84*(B5), 2161-2168.

Dieterich, J.H. (1981). Potential for geophysical experiments in large scale tests. *Geophysical Research Letters*, *8*(7), 653-656.

Dieterich, J.H. (1992). Earthquake nucleation on faults with rate- and state-dependent strength. *Tectonophysics*, *211*(1-4), 115-134.

Djiogang, F.O., Koumetio, F., Yemele, D., Konga, G.P., & Ymeli, G.L. (2022). Effect of variation of the coefficient of friction on the temperature at the level of the fault lips. *Open Journal of Earthquake Research*, *11*(3), 45-72. doi: 10.4236/ojer.2022.113004

Dongmo, M.W., Kagho, L.Y., Pelap, F.B., Tanekou, G.B., Makenne, Y.L., & Fomethe, A. (2014). Water effects on the first-order transition in a model of earthquakes. ISRN Geophysics, 2014, Article ID 160378, 7 pages. doi: 10.1155/2014/160378

Fialko, Y.A. (2004). Temperature fields generated by the elastodynamic propagation of shear cracks in the Earth. *Journal of Geophysical Research*, *109*, B01303. doi: 10.1029/2003JB002497

Florido, E., Martinez-Alvarez, F., Morales-Esteban, A., Reyes, J., & Aznarte-Mellado, J.L. (2015). Detecting precursory patterns to enhance earthquake prediction in Chile. *Computers & Geosciences*, *76*, 112-120. doi: 10.1016/j.cageo.2014.12.002

Gomberg, J., & Davis, S. (1996). Stress/strain changes and triggered seismicity at The Geysers, California. *Journal of Geophysical Research*, *101*, 733-750.

Gomberg, J., & Reasenberg, B.H. (2001). Earthquake triggering by seismic waves following the Landers and Hector Mine earthquakes. Nature, 411, 462-466.

Harris, R.A., Barall, M., Aagaard, B., Ma, S., Roten, D., Olsen, K., et al. (2018). A suite of exercises for verifying dynamic earthquake rupture codes. *Seismological Research Letters*, *89*(3), 1146-1162. doi: 10.1785/022017

Harris, R.A., Barall, M., Lockner, D.A., Moore, D.E., Ponce, D.A., Graymer, R.W., et al. (2021). A geology and geodesy based model of dynamic earthquake rupture on the Rodgers Creek-Hayward-Calaveras fault system, California. *Journal of Geophysical Research: Solid Earth*, *126*, e2020JB020577. doi: 10.1029/2020JB020577

Holcomb, D.J. (1981). Memory, relaxation, and microfracturing in dilatant rock. *Journal of Geophysical Research*, *86*(B7), 6235-6248.

Jordan, T.H., Chen, Y., Gasparini, P., Madariaga, R., Main, I., Marzocchi, W., Papadopoulos, G., Sobolev, G., Yamaoka, K., & Zschau, J. (2011). Operational earthquake forecasting: State of knowledge and guidelines for utilization. *Annals of Geophysics*,

54(4), 315-391.

Kato, N., Yamamoto, K., & Hirasawa, T. (1994). Microfracture processes in the breakdown zone during dynamic shear rupture inferred from laboratory observation of near-fault high frequency strong motion. *Pure and Applied Geophysics*, 142, 713-734.

Konga, G.P., Koumetio, F., Yemele, D., & Djiogang, F.O. (2017). One-dimensional modeling of thermal energy production in a seismic fault. *Journal of Geophysics and Engineering*, *14*.

Konga, G.P., Koumetio, F., Yemele, D., & Tanekou, G.B. (2020). Influence of viscosity on the thermal energy produced in seismic fault: One-dimensional modeling. *Annals of Geophysics*, *63*(2). doi: 10.4401/ag-8055

Kostic, S., Vasovic, N., Franovic, I., & Todorovic, K. (2014). Complex dynamics of spring-block earthquake model under periodic parameter perturbations. *Journal of Computational and Nonlinear Dynamics*, 9, 1-100.

Lachenbruch, A.H. (1980). Frictional heating, fluid pressure, and the resistance to fault motion. *Journal of Geophysical Research*, *85*(B11), 6097-6112.

Lachenbruch, A.H., & Sass, J.H. (1980). Heat flow and energetics of the San Andreas fault zone. *Journal of Geophysical Research*, *85*, 6185-6207.

Lebihain, M., Roch, T., Violay, M., & Molinari, J.F. (2021). Earthquake nucleation along faults with heterogeneous weakening rate. *Geophysical Research Letters*, *48*. doi: 10.1029/2021GL094901

Marone, C., & Saffer, D.M. (2015). The mechanics of frictional heating and slip instability during the seismic cycle. In Elsevier B.V. (Ed.), Treatise on Geophysics (2nd ed.). The Pennsylvania State University, University Park, PA, USA. doi: 10.1016/B978-0-444-53802-4.00092-0

Mase, C.W., & Smith, L. (1987). Effect of frictional heating on the thermal, hydrologic, and mechanical response of a fault. *Journal of Geophysical Research*, *92*(B7), 6249-6272.

Motchongom, M.T., Kengne, R., Tanekou, G.B., Pelap, F.B., & Kofane, T.C. (2022). Complex dynamics of a two-block model for earthquakes induced by periodic stress disturbances. *European Physical Journal Plus*, 137, 177. doi: 10.1140/epjp/s13360-022-02384-5

Noda, H., Dunham, E.M., & Rice, J.R. (2009). Earthquake ruptures with thermal weakening and the operation of major faults at low overall stress levels. *Journal of Geophysical Research, 114*. doi: 10.1029/2008JB006143

Nur, A. (1975). A note on the constitutive law for dilatancy. *Pure Appl Geophys*, *113*(1), 197-206. doi: 10.1007/BF0 1592910

Ohnaka, M., & Yamashita, T. (1989). A cohesive zone model for dynamic shear faulting based on experimentally inferred constitutive relation and strong motion source parameters. *Journal of Geophysical Research*, *94*, 4089-4104.

Ohnaka, M., Kuwahara, Y., & Yamamoto, K. (1987). Constitutive relations between dynamic physical parameters near a tip of the propagating slip zone during stick-slip shear failure. *Tectonophysics*, *144*, 109-125.

Olami, Z., Feder, J.S.H., & Kim, C. (1992). Self-organized criticality in a continuous, nonconservative cellular automaton modeling earthquakes. *Physical Review Letters*, *68*(8).

Perfettini, H., Schmittbuhl, J., & Cochard, A. (2003a). Shear and normal load perturbations on a two-dimensional continuous fault: 1. Static triggering. *Journal of Geophysical Researc*h, *108*(B9), 2408. doi: 10.1029/2002JB001804

Perfettini, H., Schmittbuhl, J., & Cochard, A. (2003b). Shear and normal load perturbations on a two-dimensional continuous fault: 2. Dynamic triggering. *Journal of Geophysical Research, 108*(B9). doi: 10.1029/2002JB001805

Ray, S., & Viesca, R.C. (2017). Earthquake nucleation on faults with heterogeneous frictional properties, normal stress. *Journal of Geophysical Research: Solid Earth*, *122*, 8214-8240. doi: 10.1002/2017JB014521

Ray, S., & Viesca, R.C. (2019). Homogenization of fault frictional properties. *Geophysical Journal*

International, *219*, 1203-1211. doi: 10.1093/gji/ggz327

Roy, M., & Marone, C. (1996). Earthquake nucleation on model faults with rate- and state-dependent friction: Effects of inertia. *Journal of Geophysical Research*, *101*(B6), 13919-13932.

Sato, H., & Fehler, M. (2009). *Seismic Wave Propagation and Scattering in the Heterogeneous Earth*. AIP Press/Springer, New York.

Schar, S., Albertini, G., & Kammer, D.S. (2021). Nucleation of frictional sliding by coalescence of microslip. *International Journal of Solids and Structures*, *225*, 111059. doi: 10.1016/j.ijsolstr.2021.111059

Scholz, C.H. (1990). *The Mechanics of Earthquakes and Faulting*. Cambridge University Press.

Scholz, C.H., Molnar, P., & Johnson, T. (1972). Detailed studies of frictional sliding of granite and implications for the earthquake mechanism. *Journal of Geophysical Research*, *77*, 6392-6406.

Sibson, R.H. (1973). Interactions between temperature and pore-fluid pressure during earthquake faulting and a mechanism for partial or total stress relief. *Nature Physical Science*, *243*, 66-68.

Tanekou, G.B., Fogang, C.F., Pelap, F.B., Kengne, R., Fozin, T.F., & Nbendjo, B.R.N. (2020). Complex dynamics in the two spring-block model for earthquakes with fractional viscous damping. *European Physical Journal Plus*, *135*(545). doi: 10.1140/epjp/s13360-020-00558-7

Terzaghi, K., Peck, R.B., & Mesri, G. (1996). *Soil Mechanics in Engineering Practice* (3rd ed.). John Wiley & Sons.

Urata, Y., Kuge, K., & Kase, Y. (2015). Effect of water phase transition on dynamic ruptures with thermal pressurization: Numerical simulations with changes in physical properties of water. *Journal of Geophysical Research: Solid Earth*, *120*, 962-975. doi: 10.1002/2014JB011370

Wang, J.H. (2016a). A dynamical study of frictional effect on scaling of earthquake source displacement spectra. *Annals of Geophysics*, *59*(2), S0210. doi: 10.4401/ag-6974

Wang, J.H. (2016b). Slip of a one-body spring-slider model in the presence of slip-weakening friction and viscosity. *Annals of Geophysics*, *59*(5), S0541. doi: 10.4401/ag-7063

Wang, J.H. (2017). Frictional and viscous effects on the nucleation phase of an earthquake. *Journal of Seismology*. doi: 10.1007/s10950-017-9680-2